Biomedicine & Pharmacotherapy 163 (2023) 114845

Contents lists available at ScienceDirect

Biomedicine & Pharmacotherapy

journal homepage: www.elsevier.com/locate/biopha

Ketoprofen, lysine and gabapentin co-crystal magnifies synergistic efficacy and tolerability of the constituent drugs: Pre-clinical evidences towards an innovative therapeutic approach for neuroinflammatory pain

Andrea Aramini [a,*], Gianluca Bianchini [a], Samuele Lillini [b], Mara Tomassetti [b], Niccolò Pacchiarotti [b], Daniele Canestrari [a], Pasquale Cocchiaro [b], Rubina Novelli [c], Maria Concetta Dragani [a], Ferdinando Palmerio [a], Simone Mattioli [b], Simone Bordignon [d], Michele d'Angelo [e], Vanessa Castelli [e], Francesco d'Egidio [e], Sabatino Maione [f], Livio Luongo [f], Serena Boccella [b], Annamaria Cimini [e,g], Laura Brandolini [a], Michele Remo Chierotti [d], Marcello Allegretti [a]

[a] R&D, Dompé Farmaceutici S.p.A, Via Campo di Pilel, 67100 L'Aquila, Italy
[b] R&D, Dompé Farmaceutici S.p.A, Via De Amicis, 80131 Naples, Italy
[c] R&D, Dompé Farmaceutici S.p.A, Via S. Lucia, 20122 Milan, Italy
[d] Department of Chemistry and NIS Centre, University of Torino, 10124 Torino, Italy
[e] Department of Life, Health and Environmental Sciences, University of L'Aquila, 67100 L'Aquila, Italy
[f] Department of Experimental Medicine, University of Campania "Luigi Vanvitelli", 80138 Naples, Italy
[g] Sbarro Institute for Cancer Research and Molecular Medicine and Center for Biotechnology, Temple University, Philadelphia, PA 19122, USA

ARTICLE INFO

Keywords:
Drug-drug co-crystal
Ketoprofen lysine salt
Gabapentin
Chronic pain
Neuropathic pain
Neuroinflammation

ABSTRACT

Chronic pain is an enormous public health concern, and its treatment is still an unmet medical need. Starting from data highlighting the promising effects of some nonsteroidal anti-inflammatory drugs in combination with gabapentin in pain treatment, we sought to combine ketoprofen lysine salt (KLS) and gabapentin to obtain an effective multimodal therapeutic approach for chronic pain. Using relevant in vitro models, we first demonstrated that KLS and gabapentin have supra-additive effects in modulating key pathways in neuropathic pain and gastric mucosal damage. To leverage these supra-additive effects, we then chemically combined the two drugs via co-crystallization to yield a new compound, a ternary drug-drug co-crystal of ketoprofen, lysine and gabapentin (KLS-GABA co-crystal). Physicochemical, biodistribution and pharmacokinetic studies showed that within the co-crystal, ketoprofen reaches an increased gastrointestinal solubility and permeability, as well as a higher systemic exposure in vivo compared to KLS alone or in combination with gabapentin, while both the constituent drugs have increased central nervous system permeation. These unique characteristics led to striking, synergistic anti-nociceptive and anti-inflammatory effects of KLS-GABA co-crystal, as well as significantly reduced spinal neuroinflammation, in translational inflammatory and neuropathic pain rat models, suggesting that the synergistic therapeutic effects of the constituent drugs are further boosted by the co-crystallization. Notably, while strengthening the therapeutic effects of ketoprofen, KLS-GABA co-crystal showed remarkable gastrointestinal tolerability in both inflammatory and chronic neuropathic pain rat models. In conclusion, these results allow us to propose KLS-GABA co-crystal as a new drug candidate with high potential clinical benefit–to–risk ratio for chronic pain treatment.

1. Introduction

Chronic pain is a complex condition that exerts an enormous personal and economic burden [1] for which an effective therapy is often not available [2]. Based on its etiology, chronic non-cancer pain is usually classified as inflammatory, neuropathic or neuroplastic.

* Corresponding author.
E-mail address: andrea.aramini@dompe.com (A. Aramini).

https://doi.org/10.1016/j.biopha.2023.114845
Received 7 April 2023; Received in revised form 29 April 2023; Accepted 4 May 2023
Available online 9 May 2023

Although their peripheral processes are different, all three types of pain have common central pathophysiological mechanisms which can converge over time [3]. Inflammatory pain can induce peripheral sensitization and neuroinflammation (i.e., inflammation localized within the nervous system) [4], the maintenance of which is associated with central sensitization and neuropathic pain. Thus, neuropathic pain is a chronic pain state that can involve both inflammatory and neuropathic components [5]. Due to the multifactorial pathophysiology of neuropathic pain, most of the existing single-target monotherapy approaches are inadequate for its treatment [6]. Combination therapies using analgesics with different mechanisms of action [7] are becoming increasingly popular for its therapeutic management [8,9]. However, multimodal analgesia is primarily achieved only using open or fixed-dose combinations of drugs in the current clinical landscape [10], which can lead to decreased compliance, suboptimal dosing/overdosing and increased side effects [11,12].

Co-crystallization is an innovative novel system of drug combination that can be used to achieve multimodal therapy [13]. Co-crystallization allows the aggregation of two or more different chemical entities through non-covalent interactions in a single, unique crystal structure, the co-crystal [14]. In pharmaceutical co-crystals, the active pharmaceutical ingredient (API) can be combined with a non-active former to improve the physicochemical and biopharmaceutical properties of the API [15], or with another (or more) API (drug-drug co-crystals) to combine the pharmacological effects and change the solid-state properties of the parent solids [16] without altering the chemical identity of the native molecules [17]. Interestingly, drug-drug co-crystals can also modify constituent APIs pharmacokinetics and physicochemical characteristics, such as solubility and dissolution rate, bioavailability, biochemical stability, and permeability [18]. This can lead to synergistic therapeutic effects between the co-formers [13] that are greater than those achieved with the simple combination of the constituent APIs by concomitant administration or fixed-dose combination of the drugs [19].

Among the nonsteroidal anti-inflammatory drugs (NSAIDs), ketoprofen is widely used for the treatment of acute inflammatory and painful conditions [20] and is usually marketed as a salt with lysine (ketoprofen lysine salt, KLS), or other counterions, to improve its physicochemical and pharmacological profile [21–23]. Gabapentin, on the other hand, is an anti-epileptic (alpha2/delta blocking) agent that has potent central and peripheral anti-allodynic activity in neuropathic pain [24,25]. Previous studies have reported that gabapentin can exhibit synergistic therapeutic effects in vivo when used in combination with NSAIDs [26–28], showing increased anti-nociceptive effects at the peripheral level in models of inflammatory pain [27,28] and anti-hyperalgesic effects at the spinal level in a rat model of postoperative pain [26]. However, whether and how the combination of ketoprofen and gabapentin could improve the anti-nociceptive effects and ameliorate the safety profile of single drugs, has not been investigated yet.

Thus, with the aim to develop a new potential therapeutic strategy for the treatment of chronic pain, in this study we first investigated whether the combination of KLS and gabapentin can lead to synergistic effects in in vitro models, and, subsequently, we synthesized a novel ternary salt co-crystal of R,S-ketoprofen, D,L-lysine and gabapentin ($LYS^{+}KET^{-}$·GABA salt co-crystal, henceforth KLS-GABA co-crystal). We then investigated the physicochemical and pharmacokinetic characteristics of the co-crystal, its effects in relieving inflammatory and neuropathic pain as well as its gastrointestinal tolerability in vivo, and elucidated aspects of its mechanisms of action.

2. Materials and methods

2.1. Evaluation of protein kinase C epsilon type (PKCε) membrane translocation

F11 hybridoma cells (ECACC 08062601) were chosen as a model of DRG neurons and cultured as previously described [29]. Following neuronal differentiation, differentiated F11 cells were treated for 24 h with paclitaxel (Sigma-Aldrich, T7402, 10 nM final concentration) to obtain a neuropathic pain in vitro model, and with KLS (Dompè Farmaceutici S.p.A., 800 μM), gabapentin (Dompé Farmaceutici S.p.A., 800 μM) and the combination of the two drugs. Translocation of PKCε from the cytoplasm to the plasma membrane was visualized as previously described [25]. Neurons in which intensity at the cell membrane was at least 2.0x greater than the mean of cytoplasmic intensity were counted as positive. In order to improve data reproducibility and signal/noise ratio, a very large number of cells were counted (at least 3–4 coverslips per culture). All experiments were analyzed in blind conditions.

2.2. In vitro gastric mucosa model with NCI-N87 cells

NCI-N87 cells (ATCC, USA) were used as a model of gastric mucosa and cultured as previously described [30]. Cells were treated for 24 h with 6% ethanol (Sigma), KLS, gabapentin and the combination of these drugs with ethanol. KLS and gabapentin stock solutions (25 mM) were freshly prepared by dissolving the powder in sterile water and then used at the final concentration of 800 μM diluted in cell culture media. Cell viability, cell index, cytotoxicity in live cells, immunofluorescence, RT-PCR, western blotting and ELISA analyses were then performed as described in the Supporting Information.

2.3. Synthesis and characterization of the co-crystal of ketoprofen, lysine and gabapentin

The co-crystallization experiments were performed by applying techniques of kneading, slurry, and controlled evaporation precipitation by direct and indirect antisolvent addition. All techniques were performed at various stoichiometric ratios in the range of 0.5–2 equivalents of gabapentin. To obtain the co-crystal of ketoprofen (KET), lysine (LYS) and gabapentin, ketoprofen lysinate (KLS) (3.028 g, 1.05 eq.) and gabapentin (1.233 g, 1.0 eq.) were dissolved in 60 mL of boiling methanol. The clear solution was cooled to room temperature, filtered and then added to 240 mL of THF under stirring. The solid precipitation took place in 30 min and the suspension was stirred at room temperature for 5 h. The solid product was isolated by vacuum filtration on a paper filter, washed with methanol (2 ×10 mL) and then squeezed under a nitrogen flow for 10 min. The solid was gently ground and then dried at 40 °C and 30 mbar overnight yielding 3.57 g of the desired product as a white solid (yield: 87%).

2.3.1. X-ray powder diffractometry (XRPD) and Thermal analyses

XRPD experiments were performed on a powder X-ray diffractometer (Rigaku Mini-Flex600) using Cu Kα radiation (1.540598 Å). Samples were scanned with a step size of 0.01° (2θ) and speed 10.0°/min (2θ) from 3° to 40° 2θ. The tube voltage and amperage were 40 kV and 15 mA, respectively.

Thermal analyses were carried out using the Mettler Toledo TGA/DSC1. Samples were weighed in an aluminum pan hermetically sealed with a pierced aluminum cover. Samples were heated from 25 °C to 320 °C at 10 °C/min.

2.3.2. Physicochemical characterization and super-saturation assessment

The main physicochemical properties of the compounds were determined by using the Sirius T3 apparatus (Pion Inc. Ltd., East Sussex, UK) equipped with an Ag/AgCl double junction reference pH electrode, a Sirius D-PAS spectrometer and a turbidity sensing device. The titration

experiments were conducted in 0.15 M KCl solution (ISA water) under a nitrogen atmosphere at a temperature of 25 ± 1 °C. All tests were performed using standardized 0.5 M KOH and 0.5 M HCl as titration reagents. The pK_as were determined by potentiometric titration in a 1.8–12.2 pH range using accurately weighted samples (1–2 mg) dissolved in 1.5 mL ISA water. The solubilities were determined by potentiometric titration in a 1.8–12.0 pH range using accurately weighted samples (10–15 mg) dissolved in 1.5 mL ISA water. Solubilities were obtained using both the Sirius T3 Curve fitting method and the Chasing Equilibrium method [31].

2.3.3. Imaging-based characterization of molecular aggregates

Molecular aggregation shape and counts of the aggregates were measured with the Ipac 2 image analyzer (Occhio s.a.). A certain sample volume was pumped through the measuring cell and irradiated with monochromatic, collimated (parallel aligned) light (λ = 440 nm). Images were taken with a high-resolution camera fitted with a motorized telecentric lens, processed, and analyzed with Callisto 3D software. The compounds were dissolved in PBS1X at 800 mg/mL and molecular aggregate sizes from 0.3 to 1000 μm were measurable depending on the focus adjustment and the mounted spacer. A syringe diameter of 2060 μm, cell thickness 100 μm, analysis quantity 0.05 mL was used. The Flow Cell calculated the particle size distribution based on the size of each detected particle.

2.4. Blood-brain barrier permeation in vitro

Ketoprofen and gabapentin BBB penetration was assessed in a human blood-brain barrier model derived from induced pluripotent stem cells [32]. KLS-GABA co-crystal (1.4 mg) and KLS+GABA mixture (1.4 mg) were added directly to the apical compartments of Transwell™ plate and ketoprofen and gabapentin penetration was assessed at 30, 60 and 90 min. The compound concentrations were determined by LC-MS/MS. The integrity of the cell layers was assessed by measuring the trans-endothelial electrical resistance (TEER) and by monitoring Lucifer Yellow (LY) permeation. Propranolol and prazosin were included as highly permeable compound and as substrate of the efflux pump BCRP, respectively.

2.5. Permeability in Caco-2 cells

Permeability assays in Caco-2 cells were performed according the protocol described in https://www.eurofinsdiscoveryservices.com/catalogmanagement/viewItem/A-B-permeability-Caco-2-pH-6.5–7.4/3318. The test compounds (mixture or the co-crystal) were tested at 100 or 400 μM and the permeability was assessed after 120 min of incubation.

2.6. Pharmacokinetic and pharmacology studies

2.6.1. Animals

Male Sprague Dawley rats (body weight 270–280 g at the time of the treatment) were used for the pharmacokinetic and BBB penetration studies. The animals were originally supplied by Charles River Laboratories, Italia S.p.A., Italy. Male Wistar rats (270–280 g) (Envigo, Italy) 8 – 9 weeks of age were used for in vivo pharmacology studies. Animals were housed 2–3 per cage under controlled illumination and standard environmental conditions for at least 1 week before experimental use. Rat chow and tap water were available ad libitum. The experimental procedures were approved by the Ministry of Health of Italy (approval number 30/2021-PR) and the Animal Ethics Committee of University of Campania "Luigi Vanvitelli". Animal care was in compliance with Italian Legislative Decree (D.L. 116/92) and European Commission Directive (O.J. of E.C. L358/1, 18/12/86) regulations on the protection of laboratory animals. All efforts were made to minimize animal suffering and the number of animals used.

2.6.2. Drug administration

In all in vivo studies, test compounds were orally administered to rats in gelatin capsules size 9 (Torpac®). Vehicle 1 (Torpac capsule filled with cellulose amid), KLS, gabapentin, KLS+GABA, KLS-GABA co-crystal and gabapentin powder were provided by Dompé Farmaceutici S.p.A. Capsules were individually filled, weighed with the substances and closed. At the day of experiment, capsules were administered through a stainless-steel dosing applicator provided by Torpac®.

2.6.3. Pharmacokinetic study and blood brain barrier permeation in vivo

Pharmacokinetic parameters were evaluated after single oral administration of KLS-GABA co-crystal and KLS+GABA mixture at a dose of 17.5 mg/kg in one gelatin capsule/animal (n = 4 rats/compound). After administration, blood (approximately 250 μL) was sampled from retroorbital plexus at the following timepoints: 30 min, 1, 2, 3, 6, 8 and 24 h after dosing.

To evaluate the blood brain barrier permeation of ketoprofen and gabapentin in vivo, ketoprofen and gabapentin brain and plasma levels were evaluated by LC-MS/MS after single oral administration of substances (KLS-GABA co-crystal and KLS+GABA mixture) in two gelatin capsules/animal at a dose of 53 mg/kg. After 2 and 24 h, animals were sacrificed, and blood and brain were collected.

2.6.4. Carrageenan-induced rat paw edema model

Peripheral inflammatory pain was induced in the left hind paw of each animal by a single intraplantar injection of 1% λ-carrageenan (100 μL for each rat in 0.9% NaCl) (Sigma- Aldrich, St. Louis, MO) as previously described [33]. KLS dose was selected based on the anti-inflammatory and analgesic activity reported in the literature in different models of pain [34,35], while the dose of gabapentin was calculated accordingly based on the co-crystal stoichiometry ratio, 1:1:1. Vehicles or drugs were orally administered 1 h before (preventive study) or 1 h after (therapeutic study) the carrageenan injection. For the preventive study, a total number of 108 animals were divided into 7 experimental groups (n = 14–16 per group): vehicle 1 (Torpac capsules filled with Avicel PH101, 2 cps), vehicle 2 (ethanol/0.9% saline, 1:19, 100 μL), indomethacin (10 mg/kg, 100 μL) in vehicle 2, KLS (47.1 mg/kg, 1 cps), gabapentin (20.4 mg/kg, 2 cps), KLS+GABA mixture (47.1 +20.4 mg/kg, 2 cps) and KLS-GABA co-crystal (67.5 mg/kg, 2 cps). For the therapeutic study, a total number of 48 animals were divided into the 7 experimental groups (n = 4 in each vehicle group and n = 8 in each treatment group). The increase in paw thickness was measured by Plethysmometer (Ugo Basile, Varese, Italy) or a digital Vernier caliper, before (0 h) and after injection of carrageenan at different time points. Edema was expressed as previously described [36]. Behavioral evaluations were performed at time 0 before the carrageenan injection and at 2, 4, 6, and 8 h post-carrageenan (1, 3, 5 and 7 h post-drug). At the end of the experiments, the animals were sacrificed with a lethal dose of urethane and paws and stomachs were dissected for morphological and biochemical evaluations.

2.6.5. Chronic constriction injury (CCI) model in rats

For this model, a total number of 52 animals were divided in 8 experimental groups (n = 4 in each sham/vehicle group and n = 8 in each treatment group): sham, vehicle 1 (pyrogen-free water), vehicle 2 (torpac capsules filled with cellulose amid, 2 cps), gabapentin 100 mg/kg (dissolved in sterile and pyrogen-free water), KLS (8.14 mg/kg, 1 cps), gabapentin (3.47 mg/kg, 1 cps), KLS+GABA mixture (8.14 +3.47 mg/kg, 1 cps) and KLS-GABA co-crystal (11.60 mg/kg, 1 cps).

Chronic constriction of the sciatic nerve was performed according to the method of Bennett and Xie [37]. Control rats underwent a sham procedure by exposure of the sciatic nerve without ligature. Vehicles or drugs were administered once a day, by oral route, in solutions (gabapentin) or in capsules from day 3 to day 10 post-CCI, and behavioral evaluations were performed at baseline (0) and at 3, 7 and 10 days post-CCI.

2.6.6. Mechanical allodynia

Mechanical allodynia was assessed using the up and down method [38] using von Frey filaments for rats (Stoelting, Wood Dale, IL, ranging from 4 g to 100 g bending force) as previously described [39]. The threshold was captured as the lowest force (*g*) that evoked scratching or licking of the stimulated hind-paw. Animals were tested at baseline (0 h) before the carrageenan injection and at different time points post-carrageenan. Responses to drugs were reported as percentage maximal effect (% MPE) as previously described [40]. The dose that produced 50% of MPE (ED50) was calculated from the linear regression analysis of the curve obtained by plotting log dose vs % MPE.

2.6.7. Thermal and mechanical hyperalgesia

Thermal hyperalgesia was evaluated using the hot plate test as described by Eddy and Leimbach [41], while mechanical hyperalgesia was determined using the Randal-Selitto paw pressure technique [42] by measuring the hind paw withdrawal threshold to a noxious mechanical stimulus (PWT). The stimulus intensity (in grams) that induced paw withdrawal from mechanical stimulation, struggle reaction, or vocal response from the animal was assessed.

2.6.8. Cytokine assay in rat spinal cord tissue

Rat paw tissues were homogenized in ice-cold PBS (1:9. v/w) to obtain a homogenate suspension. Supernatants were then removed, and levels of cytokines (IL-1β, TNF-α and IL-6) and PGE2 were quantified by enzyme-linked immunosorbent assay (ELISA) according to the protocol supplied by the manufacturer (Elabscience Biotechnology Inc. Huston. Texas. USA or R&D Systems. Minneapolis. MN. USA).

2.6.9. Evaluation of macroscopic gastric mucosal lesions

At the end of behavioral experiments, all animals were sacrificed with a lethal dose of urethane, and stomachs were removed. Ulcerogenic activity in stomachs was then evaluated using the modified method of Yamaura et al. Gastric lesions in each rat were evaluated under a dissecting microscope with square–grid eye by an arbitrary scale as follows: 0: no lesion, 1: hemorrhage erosion and damaged mucosa, 2: from 1 to 4 lesions under 3 mm, 3: over 5 lesions under 3 mm or a single lesion above 3 mm, 4: over 2 lesions above 3 mm, 5: lesions with pore. After ulcerogenic evaluation, n = 4 stomachs/group were snap-frozen and used for western blotting and ELISA assays. The other n = 4 stomachs/group were fixed in 4% buffered formaldehyde for histological and immunohistochemical analysis.

2.6.10. Histological analysis and evaluation of inflammatory mediators in stomachs

For histological analysis, stomach specimens were frozen in Optimal Cutting Temperature compound (OCT) and sliced into 12 μm thick sections by cryostat (Thermo, USA). Samples were then stained with hematoxylin (diluted 1:5 in double-distilled water) for 5 min, washed in double-distilled water and tap water, stained with eosin for 15 s, and washed again in double-distilled water and tap water. Alternatively, samples were soaked in double-distilled water, stained with Toluidine blue Working Solution for 5 min and washed in double-distilled water, 2 changes for 3 min. For mucin expression analysis, frozen sections were incubated in a 0.3% hydrogen peroxide solution for 10 min and then in PBS 0.3% Triton X-100, 4% BSA for 1 h at RT. Sections were then incubated overnight at 4 °C with mouse monoclonal anti-Mucin (1:100, ab3649, Abcam, UK). After incubation for 2 h at RT with goat anti-mouse IgG-HRP, 1:10000 in PBS containing 0.3% Triton X100, immuno-complexes were revealed using 3,3′-diaminobenzidine (SIGMAFAST DAB with Metal Enhancer, Sigma) as the chromogen. After extensive washing, sections were dehydrated and mounted using Eukitt mounting medium and observed with Zeiss Axio Imager A2.

For western blotting analyses, the whole stomachs were subjected to cycles of sonication (3 s) on ice in order to extract the proteins and then centrifuged at 4 °C. The protein concentration was evaluated using a BCA kit. Protein lysates (20 μg) were separated on precast 8–12% SDS-polyacrylamide gel and electroblotted onto polyvinyldifluoride membrane (PVDF; Sigma-Aldrich). Membranes were then incubated overnight at 4 °C with rabbit COX-1 (1:500; ab109025, Abcam) and rabbit COX-2 (1:500; ab179800, Abcam) diluted in the blocking solution. As secondary antibodies, peroxidase-conjugated anti-rabbit or anti-mouse IgG (1:10000; Vector Laboratories) were used. Immunoreactive bands were visualized by Pierce ECL Substrate (ThermoFisher Scientific). The relative densities of immunoreactive bands were determined and normalized upon tubulin (Abcam), using ImageJ software. Values were given as RU.

The active form of NFκB in gastric specimens was evaluated using the ELISA assay (ab133112, Abcam). Briefly, nuclear extracts from tissue were prepared, and the protein concentration was evaluated. The Complete Transcription Factor Binding Assay Buffer was added to each sample and loaded in each well and incubated for 1 h. Samples were incubated for 1 h with NFκB antibody followed by the goat anti-rabbit HRP conjugate. Data were analyzed using Graphpad and expressed as ng/mL. IL-8 amount was evaluated using a rat IL-8 ELISA kit from MyBioSource (#MBS9141543). Briefly, the samples were lysed, and the protein amount was quantified using a BCA assay. The standard curve was prepared following the manufacturer's instructions. 100 μL of sample or standards were added to the appropriate number of wells in the supplied plate and then 50 μL of Enzyme Solution were added to each well except the blank well. After gentle mixing, the plate was covered and incubated 1 h at 37 °C in a humid chamber. After extensive washes with the wash solution, 50 μL of Substrate A and 50 μL of Substrate B were added and incubated for 12 min at room temperature covered with foil. Lastly, 50 μL of Stop Solution was added to each well, mixed, and immediately read at 450 nm in a microplate reader (Spark, Tecan). The calculation of competitive ELISA results was performed following the manufacturer's instructions.

2.7. Data analysis

Data were analyzed using GraphPad Prism software version 9.4.0. Data from all behavioral experiments are expressed as mean ± SEM. Two-way ANOVAs followed by Tukey's post hoc tests were used to analyze differences between groups, using treatment and testing time as factors in the analysis. One-way ANOVAs followed by Dunnett post hoc comparisons or Kruskal-Wallis and post hoc Dunn's test were used to assess differences within (post-drug vs pre-drug) or between groups (using treatment as factor in the analysis) for behavioral evaluations. One-way ANOVAs followed by Dunnett post hoc comparisons were also used to assess significant differences between groups for cytokine level measurements. The level of significance was set at $P < 0.05$.

3. Results

3.1. In vitro proof-of-concept of KLS and gabapentin supra-additive effects in the modulation of key pathways in neuropathic pain and gastric mucosal damage

3.1.1. Ketoprofen potentiates gabapentin-induced inhibition of protein kinase C epsilon translocation in F11 cells

The exact mechanism by which gabapentin leads to relief of neuropathic pain is still unclear. Recent studies have demonstrated that in peripheral neurons exposed to pro-nociceptive peptides, gabapentin can act by inhibiting the membrane translocation of the noxious effector protein kinase C epsilon (PKCε) [25], and notably, gabapentin and paracetamol showed an additive behavior in mediating this inhibition [25]. Here, we analyzed the effects of KLS and gabapentin, given alone or in combination, on PKCε membrane translocation in an in vitro model of paclitaxel-induced nociception in F11 cells. Immunofluorescence analysis showed no PKCε activation in neurons in control conditions, while significant PKCε membrane translocation was induced following

paclitaxel exposure (Figs. S1A, B and C). While KLS alone did not inhibit the effect of paclitaxel, gabapentin moderately reduced it, showing an inhibition comparable to that previously described [25]. Importantly, the combination of KLS and gabapentin (KLS+GABA) significantly inhibited PKCε translocation induced by paclitaxel, exerting the strongest effect (Figs. S1A, B and C) and thus indicating a potential synergistic effect of the two drugs on a key pathway of the neuroinflammatory cascade and maintenance of pain.

3.1.2. Gabapentin improves ketoprofen tolerability in gastric epithelium by inhibiting stress-induced inflammatory and oxidative pathways and inducing mucosal repair mechanisms

NSAIDs treatment is typically associated with an increased risk of gastric erosion and ulceration, and combination with other pain modulators, such as gabapentin, has been shown to be effective in alleviating NSAID-induced adverse effects [43]. By using an in vitro model of the gastric epithelium, we investigated whether and through which mechanisms gabapentin could improve ketoprofen's gastrotolerability profile. Although the presence of lysine has been previously reported to protect against stress and NSAID-induced gastric damage [30,44,45], to study the potential gabapentin-driven protective mechanisms, we chose a KLS concentration known to still significantly reduce gastric cell viability and to potentiate EtOH-induced damage. The viability of NCI-N87 cells was analyzed following different treatments (Fig. S2A). EtOH challenge significantly reduced cell viability, and neither gabapentin nor KLS improved it in these experimental conditions. On the contrary, the combined treatment with KLS and gabapentin effectively counteracted EtOH effects (Fig. S2A). Notably, while KLS alone at the chosen concentration reduced cell viability, this effect was not observed using the KLS+GABA combination (Fig. S2A). Similar trends were observed by analyzing the cell index (i.e., cell health state) (Fig. S2B) and with a cytotoxicity assay for live-cell analysis (Fig. S2C), suggesting a marked protective effect of gabapentin against EtOH- and NSAID-induced injury.

To investigate the potential mechanisms underlying the protective effects of KLS and gabapentin combination treatment, we then analyzed the expression of a wide panel of genes involved in either mechanisms of protection or mechanisms of damage to gastric epithelium (Figs. S2D-I). The expression of genes involved in the repair and maintenance of gastric epithelium was significantly reduced by EtOH and was not affected by KLS in this setting (Fig. S2D). Gabapentin treatment instead significantly induced the expression of these protective genes, and, notably, this effect was more marked upon treatment with the KLS+GABA mixture (Fig. S2D). On the other hand, KLS was able to effectively counteract EtOH-induced upregulation of genes involved in inflammatory pathways, and these effects were further amplified with KLS+GABA mixture (Fig. S2F and G), as demonstrated in particular by the significant increase of the expression of cytoplasmic NFκB and the associated reduction of nuclear NFκB that were observed upon treatment (Fig. S2G) relative to both EtOH-stressed and control unstimulated epithelial cells.

Collectively, these data indicate that gabapentin can improve the ketoprofen gastrotolerability profile by inducing gastric mucosa repair and maintenance mechanisms and synergistically increasing the induction of anti-inflammatory signals by KLS at the gastric mucosa level.

3.2. Synthesis and characterization of KLS-GABA co-crystal

We carried out a wide screening of crystallization method with the aim to obtain a new co-crystal of R,S-ketoprofen, D,L-lysine and gabapentin (KLS-GABA co-crystal). We performed more than 100 experiments (the most representative of which are summarized in Table S1), analyzed all the collected solids via X-ray powder diffraction (XRPD) analysis and compared them with the starting materials. Kneading and slurry methods were ineffective, leading to isolation of a mixture composed of KET-LYS and gabapentin or no solid to isolate (entries 1–5, Table S1). Similarly, all experiments performed using more than one equivalent of gabapentin led to glass products or clear solutions with no solid to isolate (entries 9, 10 and 14). The best results were obtained performing several precipitation experiments by antisolvent addition with methanol as solvent and ethyl acetate or tetrahydrofuran as antisolvents (entries 7, 8 and 11, Table S1). The obtained compound had a molar ratio of 1:1:1 for KET, LYS and gabapentin, as confirmed by solution NMR (Fig. S3A). Then, the new solid phase was analysed by differential scanning calorimetry (DSC) and X-ray diffraction (XRPD) (Figs. S3B and C) and fully characterized by solid-state nuclear magnetic resonance (SSNMR) (data not shown) as a ternary salt co-crystal of ketoprofen, lysine and gabapentin (KLS-GABA co-crystal) (Scheme 1).

3.3. Physicochemical and pharmacokinetic characterization of KLS-GABA co-crystal

3.3.1. KLS-GABA co-crystal displayed higher ketoprofen solubility and systemic exposure compared to the mixture of KLS and gabapentin (KLS+GABA)

Co-crystallization can modify the physicochemical and pharmacokinetic characteristics of the APIs, such as solubility and bioavailability [18]. We analyzed the solubility of ketoprofen in KLS-GABA co-crystal relative to that in the physical mixture (i.e., open combination) of KLS and gabapentin (KLS+GABA) at pH values of blood and organs of the gastrointestinal system (i.e., stomach, ileum and colon). Interestingly, the solubility of ketoprofen in KLS-GABA co-crystal was higher compared to the simple mixture of the APIs (KLS+GABA) at all tested pH values, with an impressive 4.2-fold increase at gastric and colon pH values. To further elucidate this effect, we studied the ketoprofen solubility profile in both the co-crystal and the mixture for up to 5 h in gastric fluid (Fig. 1A). In the mixture, the solubility of ketoprofen increased and remained stable for about 2 h, ultimately decreasing and reaching a very low final concentration of ketoprofen (Fig. 1A, green line). Although following a similar trend, the maximum solubility of ketoprofen in KLS-GABA co-crystal was more than two-fold higher compared to the mixture (5.5×10^{-3} M vs 2.2×10^{-3} M), and, notably, the concentration peak was maintained for about 4 h, thus lasting much longer when compared to that observed with the mixture (3.8 h vs 2.1 h) (Fig. 1A, yellow line) and indicating a supersaturation process.

To further investigate the significance of the supersaturation phenomenon, we evaluated the 3D aggregation state of KLS, KLS-GABA and KLS+GABA solutions and compared both the number and shape using an Ipac 2 image analyzer (Occhio s.a.). With KLS and KLS+GABA solutions, we observed the presence of spherical aggregates with an average inner diameter ranging from 17.56 to 86.12 μm and from 21.40 up to 54.75 μm, respectively, and an average concentration of particles/μL of 363 and 17, respectively (Fig. 1B). In contrast, analysis of KLS-GABA co-crystal showed a background that was similar to that of milliQ water (Fig. 1B), indicating no particle aggregation in the co-crystal solution, and thus confirming a different aggregation state compared to the mixture and KLS alone that accounts for a substantial change to the physicochemical properties.

We then evaluated the impact of co-crystallization on the pharmacokinetic properties of the two drug components. Gabapentin displayed the same pharmacokinetics in both co-crystal and mixture (orally administered at 17.5 mg/kg to male Sprague Dawley rats [n = 4]). In contrast, a modest but significant increase of ketoprofen systemic exposure parameters, Cmax and AUClast, was observed with the co-crystal compared to the mixture (Cmax, 13,200 ± 3160 vs 9770 ± 2500, respectively) (AUClast, 166,000 ± 17,000 vs 126,000 ± 20,900, respectively), with a statistical significance achieved for AUClast ($P = 0.025$) (Fig. 1C and D). Notably, these results nicely fit with the reported solubility increase and supersaturation effect observed at the gastric and ileum pH and demonstrate that KLS-GABA co-crystal has unique physicochemical and pharmacokinetic characteristics that ultimately lead to a higher systemic exposure of ketoprofen after oral

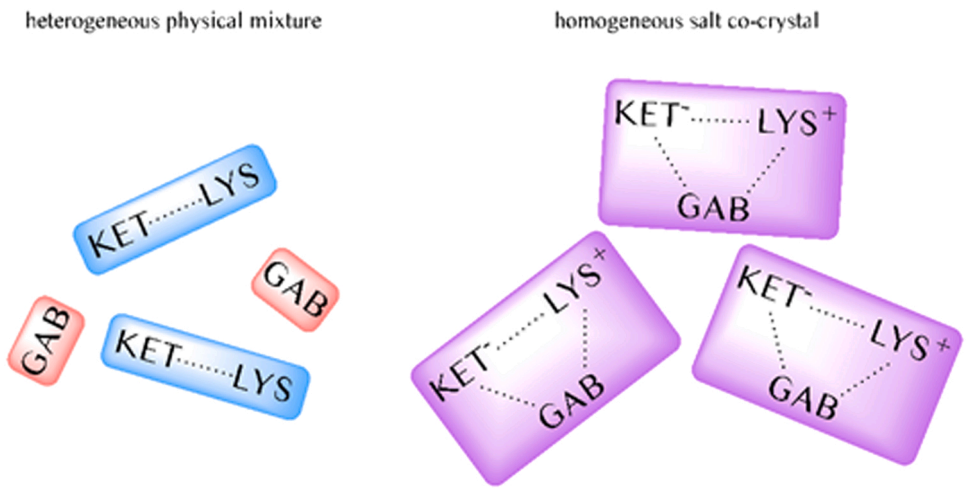

Scheme 1. Graphic representation of the difference between the heterogeneous physical mixture of KLS with GABA (KLS+GABA mixture, left) and the homogeneous crystal form of KET, LYS and gabapentin (KLS-GABA co-crystal, right). Coloured boxes represent domains of the crystal forms; dots stand for weak interactions involving the components.

administration.

3.3.2. *KLS-GABA co-crystal showed increased ketoprofen and gabapentin penetration rate in both rat and human blood-brain barrier*

Given that KLS potentiated the effect of gabapentin in the modulation of PKCε translocation, we then investigated whether a synergy could also improve the ability of gabapentin to penetrate the blood-brain barrier (BBB), thus affecting its central nervous system (CNS) distribution and its effects at the central level. To this aim, we administered KLS-GABA co-crystal or KLS+GABA mixture at oral dose of 53 mg/kg or gabapentin alone at 15.8 mg/kg to male Sprague Dawley rats (n = 4) and measured the brain to plasma ratio (% B/P). After 2 h, BBB penetration of gabapentin administered as KLS-GABA co-crystal or mixture was considerably increased compared to that observed with gabapentin alone (56.1 ± 5.1%, P = 0.033, t_4 =3.19and 58.8 ± 7.8%, P = 0.035, t_4 =3.15 vs 37.8 ± 8.5%, respectively), indicating that KLS synergistically improves the BBB penetration of gabapentin in both co-crystal and mixture. Interestingly, the % B/P of ketoprofen for the co-crystal and the mixture was also greater than that reported in the literature for the drug alone [46] (2.8 ± 0.1%, P < 0.0001, t_4 =24.20 and 2.5 ± 0.5%, P = 0.057, t_4 =5.38 vs 0.92 ± 0.09%, respectively), demonstrating that synergistic improvement in BBB penetration was observed for both KLS and gabapentin. It is worth noting that although the % B/P of both gabapentin and ketoprofen are similar for the co-crystal and the mixture, the plasma levels of ketoprofen were higher with KLS-GABA co-crystal compared to the mixture (as demonstrated by the pharmacokinetics). This suggests that a higher brain concentration for ketoprofen can be reached with the co-crystal compared to the mixture. Subsequently, we further investigated the mechanisms underlying the BBB permeability of ketoprofen and gabapentin in the co-crystal and the mixture using an in vitro model of human BBB [32]. Apparent permeability values (Papp) showed that the permeability of ketoprofen in this setting was medium, while that of gabapentin was generally low, in both directions in the co-crystal and the mixture. However, at early timepoints, both ketoprofen and gabapentin showed a higher influx ratio and a lower efflux ratio when given in the co-crystal compared to the mixture. In particular, ketoprofen influx ratio at 30 min was 1.5 ± 0.3 for the co-crystal and 0.5 ± 0.03 for the mixture (P = 0.0024, t_2 =6.2), while the efflux ratio at the same time was 0.7 ± 0.1 and 2.0 ± 0.5 for the co-crystal and the mixture, respectively (P = 0.012, t_2 =5.68); similarly, gabapentin influx ratio at 60 min was 2.1 ± 2.5 for the co-crystal and 0.4 ± 0.02 for the mixture, while the efflux ratio at the same time was 0.5 ± 0.1 and 2.8 ± 0.8 for the co-crystal and the mixture, respectively (P = 0.007, t_2 =1.17). Interestingly, at later timepoints, this phenomenon was no longer observed for gabapentin in the co-crystal, as the influx and efflux ratio were 0.55 ± 0.14 and 1.8 ± 0.9 (P = 0.034, t_2 =5.25), respectively, suggesting that gabapentin does not accumulate in the CNS long term.

Together, in vivo and in vitro BBB data indicate that KLS and gabapentin can synergistically and mutually increase the BBB penetration of each other and that co-crystallization further boosts these effects, possibly leading to a higher CNS permeation and central effects of both ketoprofen and gabapentin.

3.3.3. *KLS-GABA co-crystal showed increased permeability of ketoprofen compared to the mixture KLS+GABA in the in vitro Caco-2 cell model*

To investigate whether the co-crystallization could also boost the beneficial effects of gabapentin on ketoprofen gastrointestinal tolerability profile that we observed with the combination KLS+GABA, we determined the permeability coefficient (Papp) of ketoprofen and gabapentin in the co-crystal and the mixture in Caco-2 cells. The permeability was low for gabapentin in both the items for all concentrations (0.8 and 0.5 $cm \cdot 10^{-6}$/s for the co-crystal and 0.6 and 0.6 $cm \cdot 10^{-6}$/s for the mixture at 100 and 400 μM, respectively), while high permeability was observed for ketoprofen for all the conditions. Notably, however, the permeability of ketoprofen was significantly higher in the co-crystal (26.8 and 23.7 $cm \cdot 10^{-6}$/s at 100 and 400 μM, respectively) compared to the mixture (19.6 and 18.7 $cm \cdot 10^{-6}$/s) (P < 0.00001, t_2 =88.18 for 100 μM and P < 0.00001, t_2 =61.24 for 400 μM), suggesting another advantage of the KLS-GABA co-crystal compared to the mixture in the context of in vivo gastrointestinal tolerability. Collectively, these data prompted us to assess the potential advantages of the KLS-GABA co-crystal in a set of relevant animal models of inflammatory and neuropathic pain.

3.4. *Anti-inflammatory and analgesic properties of KLS-GABA co-crystal in an inflammatory pain in vivo model*

Considering the supra-additive effects of gabapentin and KLS in inhibiting crucial mechanisms involved in peripheral sensitization (i.e., PKCε translocation) that we observed in vitro, we first investigated the anti-inflammatory and anti-nociceptive effects of KLS-GABA co-crystal in a rat model of inflammatory pain induced by carrageenan intraplantar injection. Dose-response curves were obtained by administering increasing doses of KLS or KLS-GABA (data not shown). For each drug, the doses that produced 50% of antinociception (ED50) and its

A

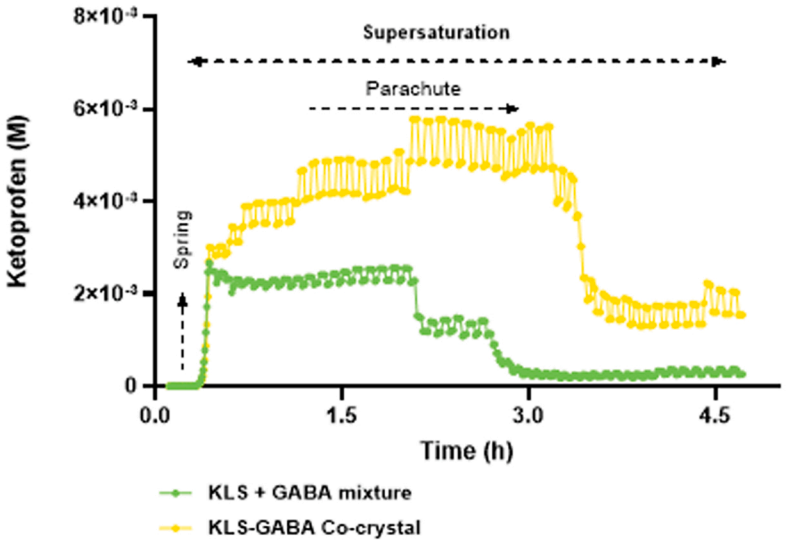

B

Species	structural shape	Diameter (μm)	Numbers of Aggregates/μL
KLS		From 17.56 to 86.12	363
KLS + GABA mixture		From 21.40 to 54.75	17
KLS- GABA Co-crystal		< 1	-
mQ water		< 1	-

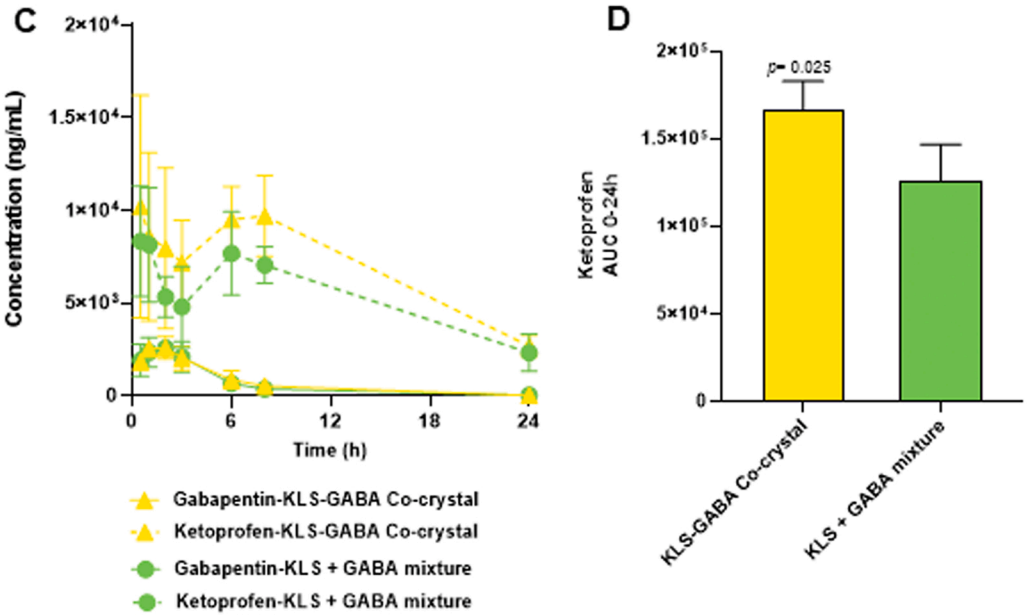

Fig. 1. A) Ketoprofen concentration profile vs time for KLS-GABA co-crystal (yellow line) and KLS+GABA mixture (green line) at 37 °C in NaCl 0.15 M water solution. B) Images acquired through the optical system Ipac 2 image analyzer (Occhio s.a.). C) Pharmacokinetics and D) AUC.

associated 95% confidence intervals (CL) were determined by linear regression analysis of the log dose–response curve. Based on these analyses, a single dose was selected for each drug and it was administered 1 h before carrageenan injection in the preventive study, and 1 h after carrageenan injection in the therapeutic study, with indomethacin, used as a reference drug [29,30].

3.4.1. KLS-GABA co-crystal has greater anti-inflammatory and anti-nociceptive effects compared to KLS, gabapentin or KLS+GABA mixture in a carrageenan-induced paw edema rat model

Carrageenan intra-plantar injection induced a time-dependent paw swelling starting from 1 h post-carrageenan injection and reaching the peak of edema after 6 h. A significant increase in the injected (left) paw volume was observed in rats treated with both vehicles used (i.e., Avicel PH101 cps or ethanol/0.9% saline, i.g.) compared to the untreated contralateral paw. The anti-inflammatory and anti-nociceptive effects of the drugs were evaluated both in a preventive (Supporting Information and Fig. S4) and a therapeutic administration setting (Fig. 2 A).

In the therapeutic setting, KLS (47.1 mg/kg, cps), given 1 h after carrageenan injection partially reduced rat paw volume compared to vehicle-treated animals at 4 h post-carrageenan and showed an anti-inflammatory effect that was similar to that of indomethacin (10 mg/kg) (Fig. 2B, C and D). Treatment with the mixture KLS+GABA caused a significant time-dependent reduction of paw volume compared to vehicle-treated group (Fig. 2B, C and D), while gabapentin alone (20.4 mg/kg, cps) had negligible effect on the increasing pattern of paw swelling (Fig. 2B, C and D). Strikingly, KLS-GABA co-crystal induced a significantly greater reduction of the paw edema compared to all the other drugs ($p = 0.02$ vs KLS, $p = 0.0008$ vs gabapentin, $p = 0.0046$ vs KLS+GABA, at 7 h post-drug) with an inhibition of paw volume of 78.10% 3 h post-drug, and these effects lasted until 7 h post-drug (Fig. 2B, C and D).

Two-way ANOVA followed by Tukey's multiple comparisons post-hoc test revealed a significant effect of time ($F_{(4, 196)} = 218.51$), treatment ($F_{(6,49)} = 60.44$) and a significant interaction time X treatment ($F_{(24,196)} = 15.78$), on paw swelling in carrageenan-treated animals.

In another set of experiments, the effects of therapeutic administration of drugs were investigated on mechanical allodynia in carrageenan-injected animals. Single oral treatment with KLS, indomethacin or KLS+GABA mixture failed to revert mechanical allodynia in carrageenan-injected rats (Fig. 2E and F), while gabapentin alone increased the withdrawal threshold compared to vehicle-injected animals at 3 h post-drug injection (Fig. 2E and F). As observed in rat paw edema and in line with the results obtained in the preventive study, KLS-GABA co-crystal exerted the greatest effects in reducing mechanical allodynia starting from 3 h and up to 5 h post-drug compared with all the other drugs ($p = 0.017$ vs KLS, $p = 0.023$ vs Indomethacin, $p = 0.012$ vs KLS+GABA, at 5 h post-drug), reaching a % MPE of 60.42 ± 5.2% at 5 h post-drug (Fig. 2E and F). Two-way ANOVA followed by Tukey's multiple comparisons post-hoc test demonstrated a significant effect of time ($F_{(4, 196)} = 102.37$), treatment ($F_{(6,49)} = 52.49$) and a significant interaction time X treatment ($F_{(24,196)} = 5.43$), on mechanical allodynia in carrageenan-treated animals.

Altogether, data from both the preventive and therapeutic studies demonstrate that KLS-GABA co-crystal has greater anti-inflammatory and anti-nociceptive effects compared to KLS and gabapentin given as single drugs and as a physical combination (KLS+GABA) and, notably, also compared to indomethacin in the described in vivo inflammatory pain model.

3.4.2. KLS-GABA co-crystal reduced neuroinflammation most efficiently compared to KLS and gabapentin given alone or in combination (KLS+GABA)

Since the carrageenan-induced inflammatory pain model is characterized by inflammation in the central nervous system (i.e., neuroinflammation) [47,48], which is mediated by the expression of cytokines that are involved in the transition from acute to chronic pain, we evaluated the spinal cord tissue expression of some neuroinflammatory markers. Levels of interleukin-1β (IL-1β), tumor necrosis factor-α (TNF-α) and interleukin-6 (IL-6) were significantly upregulated in spinal cords of animals injected with carrageenan compared to those of control rats, showing increased neuroinflammation in injured rats (Fig. 3 A - C). Treatment with KLS or gabapentin alone slightly reduced the level of IL-1β and TNFα, while a stronger reduction was observed with the mixture KLS+GABA (Fig. 3 A and B). Notably, the most significant effect in reducing the spinal expression of these cytokines was obtained with KLS-GABA co-crystal ($p = 0.0002$ and $F_{(5,18)} = 9.78$ for IL-1β;$p = 0.03$ and $F_{(5,18)} = 6.91$ for TNF-α as compared to vehicle). On the other hand, none of the treatments significantly reduced the expression of IL-6 (Figures C).

These results indicate that the therapeutic effects of KLS-GABA co-crystal in inflammatory pain could be due to its inhibition of expression of crucial neuroinflammatory cytokines in the CNS and suggest that the co-crystal could be effective also in treating neuropathic pain.

3.5. Analgesic properties of KLS-GABA co-crystal in a neuropathic pain in vivo model

We next sought to investigate the potential therapeutic effects of KLS-GABA co-crystal in a model of neuropathic pain induced by chronic constriction injury (CCI) (Fig. 4 A). In vehicle groups, CCI induced a significant reduction in paw withdrawal response (g) starting from 3 days and up to 10 days post CCI (the latest time point monitored in this study) compared to the sham group (Fig. 4B and C). Since the two vehicle groups did not differ from each other, they were merged into a single group. Treatment with KLS or with gabapentin at the dose of 3.47 mg/kg did not significantly affect the mechanical threshold of rats compared to vehicle-treated CCI group, while administration of the mixture KLS+GABA induced a moderate analgesic effect until 10 days post CCI as compared to the vehicle-injected CCI animals (Fig. 4B and C). However, mechanical allodynia was significantly reduced after repeated oral administration of KLS-GABA co-crystal as compared to all other drugs ($p = 0.0012$ vs KLS, $p = 0.0012$ vs GABA, 7 days post-drug), reaching a striking % MPE of 83.07 ± 7.43%, higher than the efficacy of gabapentin alone at 100 mg/kg that was used as reference drug [49] (Fig. 4B and C). Notably, the stronger effect of co-crystal on mechanical allodynia was still present 10 days post CCI, with mechanical threshold values that were comparable to those observed in sham animals. Two-way ANOVA followed by Tukey's multiple comparisons post-hoc test demonstrated a significant effect of time ($F_{(3, 135)} = 89.05$), treatment ($F_{(6,45)} = 18.43$) and a significant interaction time X treatment ($F_{(18,135)} = 5.79$), on mechanical allodynia in CCI rats.

To further investigate the effects of KLS-GABA co-crystal in neuropathic pain, we then assessed its potential efficacy on mechanical hyperalgesia in the same CCI model. Paw withdrawal threshold (PWT) was strongly reduced in vehicle (Avicel PH101 cps or sterile water)-treated rats on day 3, 7 and 10 post CCI as compared to sham animals (Fig. 4D). Gabapentin at 100 mg/kg reverted mechanical hyperalgesia as compared to vehicle rats, and also gabapentin at 3.47 mg/kg significantly increased PWT until 7 days post CCI (Fig. 4D). Whereas neither KLS nor, more surprisingly, the mixture KLS+GABA affected the reduced mechanical threshold in CCI rats as compared to vehicle-treated ones, the maximum anti-hyperalgesic effect was obtained with KLS-GABA co-crystal administration ($p = 0.0001$ vs KLS, $p = 0.0009$ vs GABA, $p = 0.045$ vs gabapentin, 7 days post-drug), which restored the PWT to sham group values until 10 days post CCI (Fig. 4D). Two-way ANOVA followed by Tukey's multiple comparisons post-hoc test showed a significant effect of time ($F_{(3, 135)} = 187.22$), treatment ($F_{(6,45)} = 22.39$) and a significant interaction time X treatment ($F_{(18,135)} = 9.50$), on mechanical hyperalgesia in CCI rats.

Lastly, we also tested the drugs' effects on thermal hyperalgesia after CCI. Starting from 3 days after surgery and until the end of observations

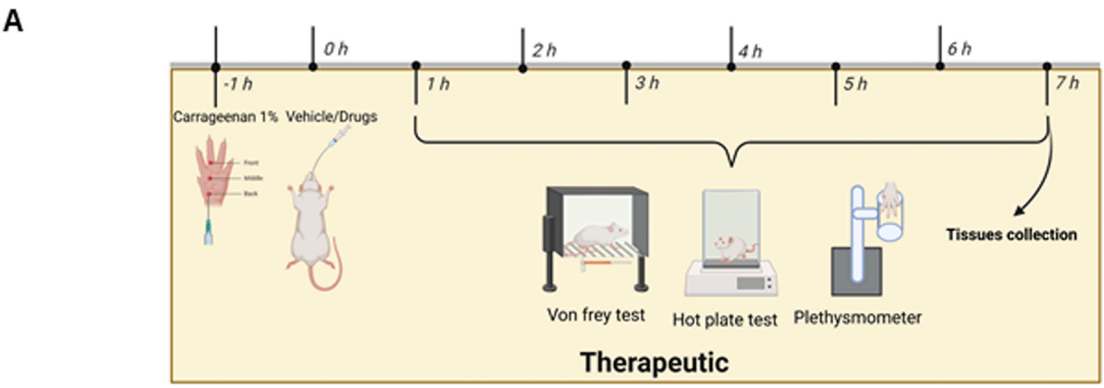

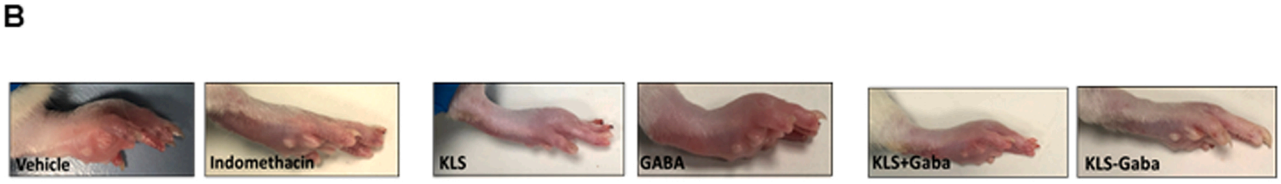

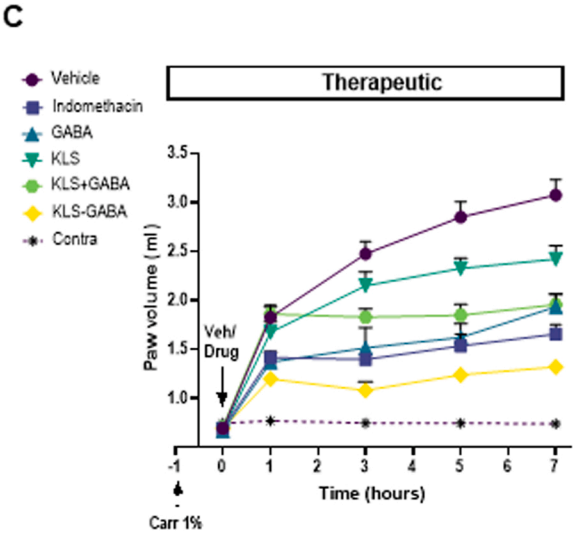

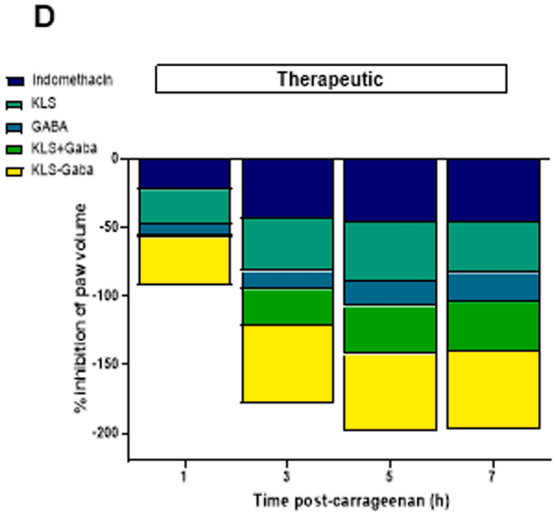

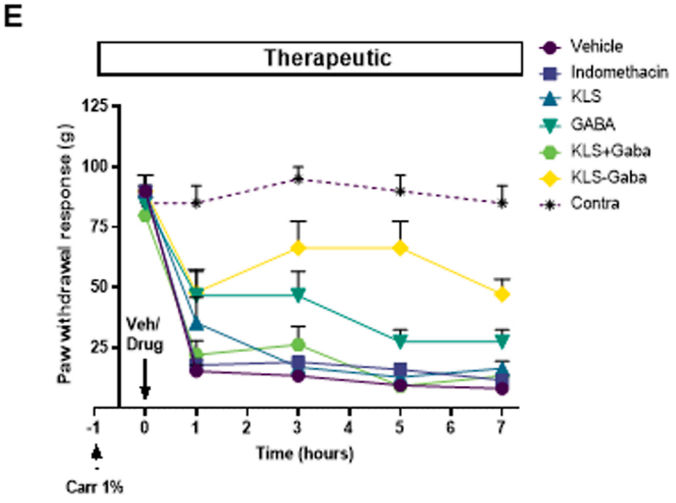

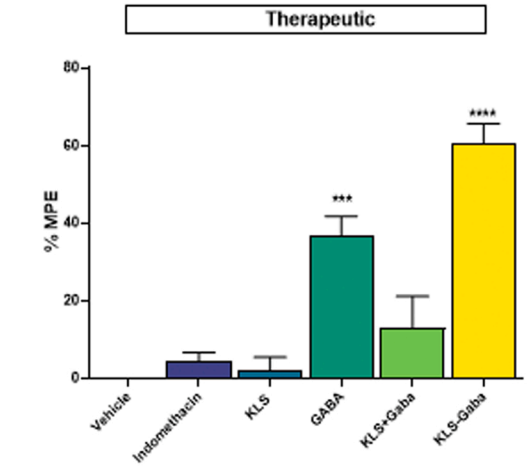

(caption on next page)

Fig. 2. A) Experimental time of therapeutic effect of vehicle or KLS-GABA co-crystal, KLS+GABA combination, KLS, gabapentin and indomethacin in carrageenan-induced edema in rat. B) Representative macroscopic photographs of paws from carrageenan-injected rats, treated with vehicle or different drugs, at 8 h post carrageenan injections (7 h post-drug). C) Time-course of anti-inflammatory effect of KLS-GABA co-crystal or KLS+GABA combination compared with KLS, GABA, Indomethacin or Vehicle on rat paw swelling (mL) injected 1 h after intra-plantar injection of 1% of carrageenan. D) % Inhibition of paw volume induced by KLS-GABA co-crystal or KLS+GABA combination compared with KLS, gabapentin, indomethacin or vehicle 1, 3, 5- and 7-hours post-drugs injection (2, 4, 6 and 8 h post-carr). E) Time-course of anti-allodynic effect of KLS-GABA co-crystal or KLS+GABA combination compared with KLS, gabapentin, Indomethacin or Vehicle on paw withdrawal response (g) injected 1 h after intra-plantar injection of 1% of carrageenan. F) % of maximum possible effect (%MPE) of KLS-GABA co-crystal or KLS+GABA combination compared with KLS, GABA, indomethacin or vehicle on mechanical allodynia. Each time point represents the mean ± SEM of 4 rats for vehicle and of 8 rats for each drug. $P < 0.05$ was considered as statistically significant and calculated by using two-way ANOVA followed by Tukey's post-hoc test. For paw swelling (C): at 1 h, vehicle showed * **$p < 0.001$ vs contra, KLS-GABA co-crystal *$p < 0.05$ vs vehicle and * **$p < 0.001$ vs KLS+GABA. At 3 h, vehicle showed * ** *$p < 0.0001$ vs contra, KLS *$p < 0.05$ vs vehicle, KLS+GABA *$p < 0.05$ vs vehicle and KLS-GABA co-crystal * ** *$p < 0.0001$ vs vehicle, * *$p < 0.01$ vs Indomethacin, *$p < 0.05$ vs KLS and * **$p < 0.001$ vs KLS+GABA. At 5 h, vehicle showed * ** *$p < 0.0001$ vs contra, indomethacin * **$p < 0.001$ vs vehicle, KLS * **$p < 0.001$ vs vehicle, KLS+GABA * *$p < 0.01$ vs vehicle and KLS-GABA co-crystal * ** *$p < 0.0001$ vs vehicle, *$p < 0.05$ vs Indomethacin and * *$p < 0.01$ vs KLS+GABA. At 7 h, vehicle showed * ** *$p < 0.0001$ vs contra, indomethacin * **$p < 0.001$ vs vehicle, KLS * *$p < 0.01$ vs vehicle, KLS+GABA * **$p < 0.001$ vs vehicle and KLS-GABA co-crystal * ** *$p < 0.0001$ vs vehicle, *$p < 0.05$ vs KLS, and * *$p < 0.01$ vs KLS+GABA. For mechanical allodynia (E): at 1 h, vehicle showed * **$p < 0.001$ vs contra, Gaba *$p < 0.05$ vs contra and *$p < 0.05$ vs vehicle, and KLS-GABA co-crystal *$p < 0.05$ vs vehicle. At 3 h vehicle showed * ** *$p < 0.0001$ vs contra, Gaba * **$p < 0.001$ vs contra and *$p < 0.05$ vs vehicle, and KLS-GABA co-crystal * *$p < 0.01$ vs vehicle, *$p < 0.05$ vs Indomethacin and *$p < 0.05$ vs KLS. At 5 h Vehicle showed * ** *$p < 0.0001$ vs contra, Gaba * **$p < 0.001$ vs contra and KLS-GABA co-crystal * **$p < 0.001$ vs vehicle, *$p < 0.05$ vs Indomethacin, *$p < 0.05$ vs KLS and *$p < 0.05$ vs KLS+GABA. At 7 h vehicle showed * **$p < 0.001$ vs contra, Gaba * **$p < 0.001$ vs contra and KLS-GABA co-crystal * *$p < 0.01$ vs vehicle, * *$p < 0.01$ vs Indomethacin, *$p < 0.05$ vs KLS and *$p < 0.05$ vs KLS+GABA.

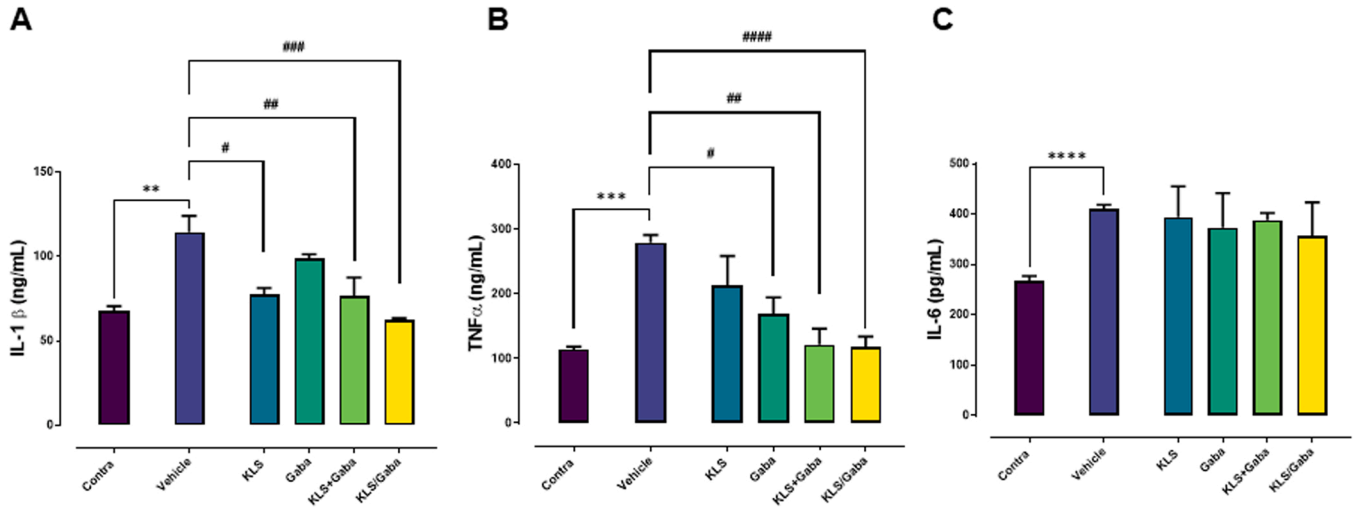

Fig. 3. Expression of neuroinflammatory mediators (IL-1β (A), TNFα (B), and IL-6 (C)) in spinal cords of carrageenan-injected rats treated with vehicle, KLS+GABA mixture, KLS-GABA co-crystal or single compounds. Analyses were carried out 6 h post-drug (7 h post-carrageenan) in 5 animals per group. $P < 0.05$ was considered as statistically significant and calculated by using one-way ANOVA followed by Tukey's post-hoc test. * *$p < 0.01$, * **$p < 0.001$ and * ** *$p < 0.0001$ vs contra, $^{\#}p < 0.05$, $^{\#\#}p < 0.01$, $^{\#\#\#}p < 0.001$ and $^{\#\#\#\#}p < 0.0001$ vs vehicle.

(10 days), paw latency significantly decreased in vehicle-treated CCI animals (Fig. 4E). KLS did not display a significant effect on thermal hyperalgesia whereas gabapentin as single administration at 100 and 3.47 mg/kg and KLS+GABA mixture significantly reduced thermal hyperalgesia and increased hot plate latency until 10 days post CCI compared to vehicles (Fig. 4E). Strikingly, KLS-GABA co-crystal induced the highest increase ($p = 0.0032$ vs KLS, $p = 0.013$ vs GABA, 7 days post-drug) in the paw latency at 7 and 10 days compared to control rats (Fig. 4E), again demonstrating its greater therapeutic efficacy compared to all tested treatments and drug combinations also studied using the in vivo model of neuropathic pain. Two-way ANOVA followed by Tukey's multiple comparisons post-hoc test showed a significant effect of time ($F_{(3, 135)} = 76.97$), treatment ($F_{(6,45)} = 36.95$) and a significant interaction time X treatment ($F_{(18,135)} = 7.79$), on thermal hyperalgesia in CCI rats.

3.6. KLS-GABA co-crystal has increased gastrointestinal tolerability compared to KLS, indomethacin and the mixture KLS+GABA

NSAID-induced gastrolesivity is a crucial limiting factor to the use of this class of drugs in chronic therapeutic regimens. As such, we investigated the gastrolesive effect of the new KLS-GABA co-crystal compared to that of KLS, gabapentin, indomethacin and the mixture KLS+GABA by analyzing the stomachs of rats used for the CCI neuropathic pain model and in the therapeutic treatment in carrageenan-induced paw edema model.

3.6.1. KLS-GABA co-crystal has lower gastrointestinal anti-ulcerogenic activity in neuropathic and inflammatory pain rat models

Histological analysis of the stomachs of CCI animals revealed that only KLS-treated rats had gastrointestinal damage, showing some hemorrhagic red spots on gastric mucosa, but no congestion, erosion or ulceration (ulcer index: 2.25 ± 0.4; $p < 0.0001$; Kruskal-Wallis statistic=37.14) (Fig. 5 A, B and C). On the contrary, injured rats treated with gabapentin at different dosages or KLS-GABA co-crystal did not display any gastric ulcerogenic signs, similarly to vehicle-treated group, with an ulcer index of 0 (Fig. 5 A, B and C).

In the carrageenan-induced inflammatory pain model, KLS treatment caused evident gastrointestinal damage, with hemorrhagic red spots on gastric mucosa, but no congestion, erosion or ulceration, with a mean value for ulcer index of 2.75 ± 0.16 ($p < 0.0001$; Kruskal-Wallis statistic=39.11) that was similar to that obtained analyzing rats

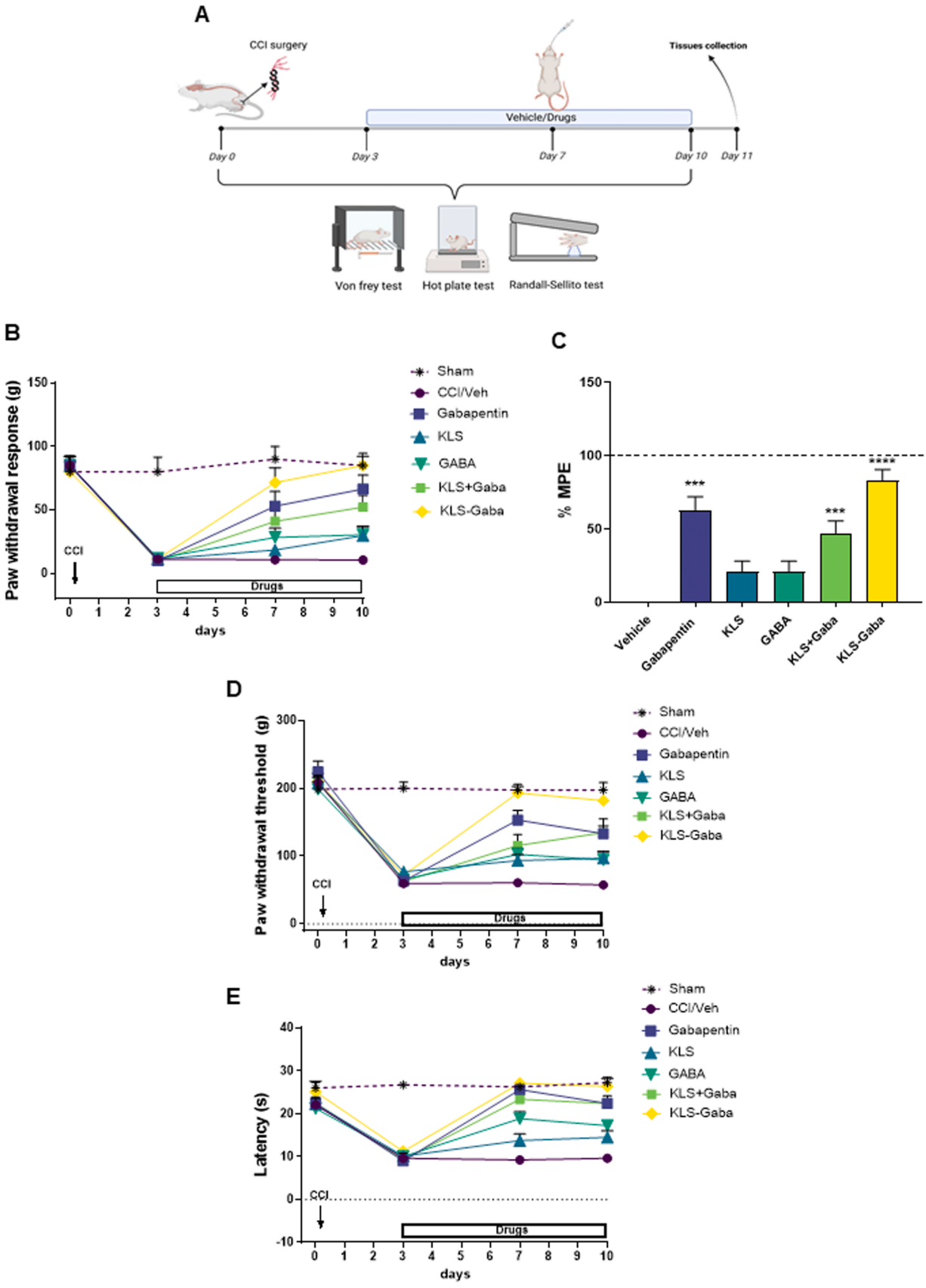

(caption on next page)

Fig. 4. A) Experimental time of effect repeated treatments of vehicle or KLS-GABA co-crystal, KLS+GABA combination, KLS, GABA and indomethacin in CCI rat. Time-course of analgesic effect of repeated treatments (7 days) with ketoprofen lysine salt (KLS), gabapentin (GABA), KLS+GABA, KLS-GABA co-crystal and Gabapentin (100 mg/kg, 100uL) compared to Vehicle-treated rats (CCI) on CCI-induced mechanical allodynia (B and C), mechanical hyperalgesia (D) and thermal hyperalgesia (E) and each time point represents the mean ± SEM of four (Sham)/eight (CCI+Veh/drugs) rats. Black arrows indicate surgery induction and empty rectangle indicate the duration of treatment. $P < 0.05$ was considered as statistical significance and calculated by using Two-way ANOVA followed by Tukey's post-hoc test for comparisons between groups. For mechanical allodynia (B and C), at 3 days, vehicle showed *$p < 0.05$ vs Sham, KLS, Gaba, Gabapentin, KLS+GABA and KLS-GABA co-crystal * *$p < 0.01$ vs Sham. At 7 days, vehicle showed *$p < 0.05$ vs Sham, KLS and Gaba * *$p < 0.01$ vs Sham, Gabapentin *$p < 0.05$ vs CCI/vehicle, KLS-GABA co-crystal *$p < 0.05$ vs CCI/vehicle and *$p < 0.05$ vs KLS+GABA. At 10 days, vehicle, KLS and Gaba showed *$p < 0.05$ vs Sham, Gabapentin and KLS+GABA *$p < 0.05$ vs CCI/vehicle, KLS-GABA co-crystal * ** *$p < 0.0001$ vs CCI/vehicle, *$p < 0.05$ vs KLS+GABA and * *$p < 0.01$ vs KLS. For mechanical hyperalgesia (D), at 3 days vehicle, KLS, Gaba, Gabapentin, KLS+GABA and KLS-GABA co-crystal showed * **$p < 0.001$ vs Sham, and Gaba *$p < 0.05$ vs KLS+GABA. At 7 days vehicle, KLS and Gaba showed * **$p < 0.001$ vs Sham, Gaba *$p < 0.05$ vs CCI/vehicle, Gabapentin * *$p < 0.01$ and KLS-GABA co-crystal * ** *$p < 0.0001$ vs CCI/vehicle and * ** *$p < 0.0001$ vs KLS. At 10 days vehicle, KLS and Gaba showed * *$p < 0.01$ vs Sham, Gaba *$p < 0.05$ vs CCI/vehicle, Gabapentin * *$p < 0.01$ vs CCI/Vehicle and *$p < 0.05$ vs Sham and KLS-GABA co-crystal * ** *$p < 0.0001$ vs CCI/vehicle, * **$p < 0.001$ vs KLS+GABA and * **$p < 0.001$ vs KLS.
For thermal hyperalgesia (E), at 3 days vehicle, KLS, Gaba, Gabapentin, KLS-GABA co-crystal and KLS+GABA showed * ** *$p < 0.0001$ vs Sham. At 7 days vehicle and KLS showed * ** *$p < 0.0001$ vs Sham, KLS * ** *$p < 0.0001$ vs KLS+GABA, Gaba * *$p < 0.01$ vs CCI/vehicle and *$p < 0.05$ vs KLS+GABA, Gabapentin * ** *$p < 0.0001$ vs CCI/vehicle, KLS-GABA co-crystal * ** *$p < 0.0001$ vs CCI/vehicle and * **$p < 0.001$ vs KLS, KLS+GABA * **$p < 0.001$ vs CCI/vehicle, *$p < 0.05$ vs KLS. At 10 days vehicle * **$p < 0.001$ vs Sham, KLS * *$p < 0.01$ vs Sham, *$p < 0.05$ vs KLS+GABA, Gaba * **$p < 0.001$ vs CCI/vehicle, * *$p < 0.01$ vs Sham and *$p < 0.05$ vs KLS+GABA, Gabapentin * ** *$p < 0.0001$ vs CCI/vehicle, KLS-GABA co-crystal * **$p < 0.001$ vs CCI/vehicle and * *$p < 0.01$ vs KLS, KLS+GABA * *$p < 0.01$ vs CCI/vehicle.

treated with indomethacin (Fig. 5D, E and F). Slight damage to the gastric mucosa was induced by KLS+GABA mixture in this model (ulcer index 1.25 ± 0.31); however,carrageenan-injected rats treated with gabapentin or with KLS-GABA co-crystal did not display any gastric ulcerogenic signs (ulcer index 0 and 0.37 ± 0.18, respectively), similar to vehicle-treated group (0) (Fig. 5D, E and F).

These data demonstrate that in both chronic and acute treatment, KLS-GABA co-crystal has increased gastrointestinal tolerability compared to the mixture KLS+GABA and, especially, KLS alone.

3.6.2. KLS-GABA co-crystal preserved gastric mucosa structure and inhibited gastric inflammation

Since the ulcer index for both the co-crystal and the mixture was higher in carrageenan-injected rats, we further analyzed stomachs from carrageenan-injected animals to investigate the molecular mechanisms underlying the improved gastrointestinal tolerability of KLS-GABA co-crystal observed with the macroscopic histologic analysis.

Mucin staining and toluidine blue analysis showed that indomethacin, KLS and KLS+GABA-treated rats had a compromised gastric mucosa structure and increased infiltration of mast cells, whereas in the gabapentin and KLS-GABA co-crystal groups, the mucosa was preserved, and mast cells infiltration was considerably lower (Fig. S5).

To further investigate the molecular aspects of the improved gastrotolerability of KLS-GABA co-crystal, we analyzed the gastric expression of the two isoforms of cyclooxygenase (COX). COX-1 protein levels were significantly decreased in gastric specimens of rats receiving indomethacin compared to vehicle-treated rats, while no effect was observed analyzing stomachs of rats receiving KLS and the mixture KLS+GABA (Fig. 5 G). On the contrary, both gabapentin and KLS-GABA co-crystal treated rats showed COX-1 protein gastric levels that were increased even compared to those of vehicle rats, thus suggesting a gastroprotective effect of these compounds (Fig. 5 G). Gastric levels of COX-2 were significantly increased following indomethacin, KLS and KLS+GABA treatments, while co-crystal KLS-GABA administration led to significantly lower COX-2 protein levels (Fig. 5 G). Modulation of gastric COX-2 levels could explain the improved gastrotolerability of this compound and suggest a reduced inflammatory effect. Such effect was confirmed by ELISA assays for the gastric expression of IL-8 and the active form of NFκB (p-NFκB), the levels of which were significantly upregulated upon indomethacin, KLS and KLS+GABA treatments compared to those of rats receiving gabapentin or KLS-GABA co-crystal, which were similar to those of vehicle-treated rats (Fig. 5H).

The absence of gastric damage upon treatment with KLS-GABA co-crystal demonstrates the ability of this compound to avoid the gastrointestinal side effects that are characteristic of NSAIDs while maintaining, and also strengthening, the typical therapeutic effects.

4. Discussion

Treatment of chronic pain is still an unmet medical need [8]. There are no approved combination therapies with clear efficacy to treat chronic pain, and the development of new effective pharmacological approaches is of the utmost importance for clinical practice and health care [50]. In this study, we demonstrated for the first time that the combination of KLS and gabapentin can lead to supra-additive therapeutic effects for pain treatment and an improved safety profile. Further, we have synthesized a new ternary complex drug-drug co-crystal of ketoprofen, lysine and gabapentin (KLS-GABA co-crystal). KLS-GABA co-crystal showed higher ketoprofen gastric solubility and permeability and increased BBB penetration of both ketoprofen and gabapentin compared to the monotherapies with the two drugs and to their mixture (KLS+GABA), and resulting in increased therapeutic efficacy in both inflammatory and neuropathic pain animal models as well as an improved gastrointestinal tolerability profile.

The most crucial aspect when studying a drug combination is the evaluation of the joint therapeutic effects and of the off-target interactions of the drugs [51]. Our in vitro data demonstrated initial proof-of-concept that KLS can improve gabapentin's analgesic effects, in not merely an additive but in a synergistic way. Previous studies have shown that paracetamol can enhance the gabapentin-mediated effects on PKCε [25]. The membrane translocation of PKCε is induced by inflammatory mediators in peripheral fibers and is crucial for pain maintenance [52], and its inhibition results in antinociceptive effects that have been recognized as an important component of gabapentin-mediated analgesia [25]. The combination of KLS and gabapentin produced a synergistic increase in the inhibition of PKCε membrane translocation greater than that observed with either KLS or gabapentin alone, indicating a potentially greater antinociceptive effect of this drug combination compared to each drug alone. In addition, the overall protection of the gastric epithelium against inflammation and oxidative stress observed with the combination of KLS and gabapentin not only confirms minimal off-target activity, but also suggests that gabapentin can ameliorate ketoprofen's gastrointestinal tolerability.

Building on these data, we report here the synthesis and characterization of a new compound with structural and chemical features of a ternary salt co-crystal, in which ketoprofen, lysine and gabapentin have a 1:1:1 stoichiometry ratio, and KLS and gabapentin interact through non-ionic bonds. KLS-GABA co-crystal is thus a unique, single-entity, solid form of ketoprofen, lysine and gabapentin, which is completely different from the simple physical mixture of these APIs.

Co-crystal forms can enable greater solubility and subsequent absorption of the constituent APIs compared to their physical combinations (mixtures) [15]. In KLS-GABA co-crystal, ketoprofen reached a significantly higher gastric solubility compared to that observed with

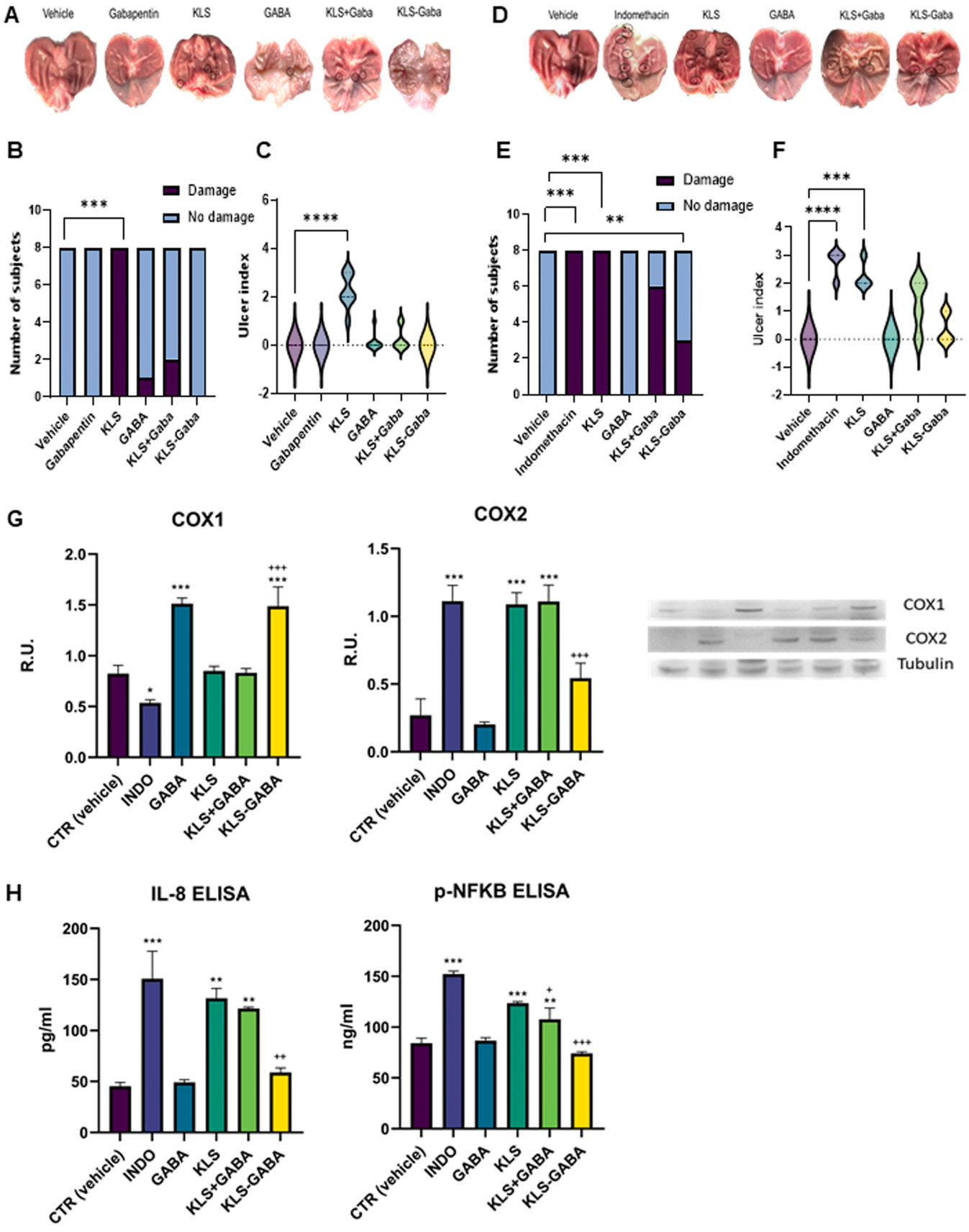

(caption on next page)

Fig. 5. Chronic treatment (CCI model) A) Representative images of ulcerogenic activity in the stomachs of CCI rats 7 days after repeated treatment with vehicle, gabapentin, KLS, GABA, KLS+GABA or KLS-GABA co-crystal. Black circles indicate areas of damaged mucous and spot lesions. B) Bar graph representing the number of CCI animals showing gastric damage 7 days after repeated treatment with vehicle, gabapentin, KLS, GABA, KLS+GABA or KLS-GABA co-crystal (n = 8 per group). $P < 0.05$ was considered statistically significant and calculated by applying Fisher's exact test. C)Violin plot representing ulcer index in CCI rats 7 days after repeated treatment with vehicle, gabapentin, KLS, GABA, KLS+GABA or KLS-GABA co-crystal (n = 8 per group). $P < 0.05$ was considered statistically significant and calculated by Kruskal-Wallis test. Acute treatment (carrageenan model). D) Representative images of ulcerogenic activity in the stomachs of carrageenan-treated rats 7 h after single administration of vehicle, indomethacin, KLS, GABA, KLS+GABA or KLS-GABA co-crystal. Black circles indicate areas of damaged mucous and spot lesions. E) Bar graph representing the number of carrageenan-injected animals showing gastric damage 7 h after single administration of vehicle, indomethacin, KLS, GABA, KLS+GABA or KLS-GABA co-crystal (n = 8 per group). $P < 0.05$ was considered statistically significant and calculated by applying Fisher's exact test. F) Violin plot representing ulcer index in carrageenan-injected animals showing gastric damage 7 h after single administration of vehicle, indomethacin, KLS, GABA, KLS+GABA or KLS-GABA co-crystal (n = 8 per group). $P < 0.05$ was considered statistically significant and calculated by Kruskal-Wallis test. G) WB analyses for COX1 and COX2 of rat gastric specimens upon different treatments. One-way ANOVA, * $p < 0.05$; * ** $p < 0.0005$ vs. CTR (vehicle); + ++ $p < 0.0005$ vs. KLS (N = 3). Stomachs were collected 7 h after the drugs administration. H) ELISA for p-NFKB of rat gastric specimens upon different treatments. One-way ANOVA, * ** $p < 0.0005$, * * $p < 0.005$ vs. CTR (vehicle); + $p < 0.05$, + ++ $p < 0.0005$ vs. KLS (N = 3). Data are expressed as ng/mL. ELISA for rat IL-8 of gastric specimens upon different treatments. One-way ANOVA, * ** $p < 0.0005$, * * $p < 0.005$ vs. CTR (vehicle); + + $p < 0.005$ vs. KLS (N = 3). Data are expressed as pg/mL. (CTR, vehicle, carrageenan), indomethacin (INDO), gabapentin (GABA), KLS, KLS+GABA, and the co-crystal KLS-GABA.

the simple mixture of KLS+GABA in terms of both concentration peak and peak lasting time, a profile that is characteristic of a supersaturation with "spring and parachute" phenomena [53,54]. Supersaturation has been described for co-crystals as a result of the high kinetic solubility of thermodynamically high-energy forms of molecules leading to soluble concentrations higher than the equilibrium solubility of the thermodynamically stable form of the drug [53,55]. The supersaturated drug solution, however, is thermodynamically unstable and tends to crystallize as the stable form of the drug, leading to a rapid decrease of concentration to the solubility level of the stable form (spring effect) [54]. The addition of excipients functioning as precipitation inhibitors, such as polymers and surfactants [56], is generally used to stabilize the supersaturation state (parachute effect) [54,57,58]. For example, polymer excipients were used to maximize oral bioavailability and leverage the therapeutic benefits of Entresto®, which is a drug-drug (valsartan/sacubitril) co-crystal currently available on the market that is used for the treatment of heart failure [58]. Interestingly, the three-component KLS-GABA co-crystal showed both spring and parachute supersaturation phenomena without the addition of any excipients, suggesting that lysine can behave as a supersaturation stabilizer. The reduced particle aggregation observed for the co-crystal compared to the mixture and the constituent drugs is consistent with the results of supersaturation studies [59], and an improved oral bioavailability of co-crystals showing the "parachute effect" has been also previously reported [54,58,59]. Together, these interconnected features of KLS-GABA co-crystal can also explain the increased in vitro permeability and in vivo oral absorption of ketoprofen in the co-crystal in comparison with the drug-drug combination.

These characteristics of the KLS-GABA co-crystal led us to predict several advantages for its therapeutic use, as they could mean higher efficacy with fewer side effects [15]. In a rat model of inflammatory pain, KLS-GABA co-crystal had the highest preventive and therapeutic efficacy, exerting greater anti-inflammatory and anti-nociceptive effects compared to monotherapies with KLS and gabapentin, their combination (KLS+GABA) and indomethacin. Similarly, in the CCI neuropathic pain model, KLS-GABA co-crystal was the most efficient in reversing mechanical allodynia and hyperalgesia, and thermal hyperalgesia in comparison with gabapentin at 100 mg/kg (reference treatment [49]), a dosage of gabapentin which was much higher than that administered through the co-crystal (3.5 mg/kg of gabapentin in 11.60 mg/kg of KLS-GABA co-crystal). Notably, data from tolerability studies in Göttingen minipigs orally treated with the co-crystal at 15 mg/kg daily for 7 consecutive days did not highlight any gabapentin-associated side effects (e.g., sedation, data not shown).

A significant reduction of the spinal expression of neuromodulators, such as TNFα and IL-1β, was observed in animals treated with KLS-GABA co-crystal in the carrageenan model experiments. This observation indicates greater efficacy of the co-crystal relative to other treatments in counteracting neuroinflammation and fits well with the supra-additive effects of KLS and gabapentin observed on PKCε translocation in vitro. Numerous studies have in fact demonstrated the coordinated role of TNFα [60], and also IL-1β, with neuronal PKCε in inducing the hyperalgesic priming in acute carrageenan-induced inflammation [61,62] and in modulating chronic inflammatory processes [63]. In a CCI model of neuropathic pain, TNFα and IL-1β were crucial factors in inducing and maintaining PKCε-mediated phosphorylation and sensitization of the transient receptor potential cation channel subfamily V member 1 (TRPV1), which is an important contributor to pain., This represents a key pathway for the acute-to-chronic pain transition and its maintenance [64] that can be targeted by KLS-GABA co-crystal.

In light of this evidence, the superiority of the co-crystal in modulating the spinal expression of these neuroinflammatory modulators, in comparison not only with single agents but also with the mixture, is consistent with the pharmacological effects obtained with the co-crystal in both inflammatory and neuropathic pain and suggests a higher central distribution of the drug components in the co-crystal form. Although BBB permeation studies failed to provide solid evidence of a significant difference between the co-crystal and the combination in this context, they clearly showed an increased central permeation of the two drugs when administered in combination versus the single components. These data, together with the differences in BBB influx/efflux rate observed in vitro in favor of KLS-GABA co-crystal and with its marked effect on spinal neuromodulation, still support the hypothesis that the striking difference in the anti-nociceptive therapeutic effect could be attributed to a change in the central localization of the drug components driven by the unique physicochemical characteristics of the co-crystal that facilitate drug-drug synergy in the peripheral and/or central nervous compartment.

Data reported here warrant additional studies to clarify the exact mechanism underlying the striking efficacy enhancement associated with the co-crystallization. However, our results outline a clear mechanistic picture for the observed gastroprotective effect. *In vitro* data clearly show the ability of gabapentin to stimulate gastric mucosa repair and protection pathways, and the combination of KLS+GABA markedly decreased the stress-induced pro-inflammatory signals. In particular, the ability of the drug-drug combination to synergistically inhibit the constitutive NFκB nuclear expression in gastric mucosa fits well with findings from *ex vivo* studies. Indeed, in gastric biopsies from animals treated with the KLS+GABA mixture, and more evidently with the KLS-GABA co-crystal, the NSAID-induced upregulation of NFκB and the consequent upregulation of IL-8 and COX-2 were significantly inhibited. *Ex vivo* results with co-crystal also showed how the downregulation of COX-2 expression was coordinated with an increased expression of the constitutive COX-1 protein, which is fundamental for the biosynthesis of prostaglandins responsible for the protection of mucosal barrier. Its inhibition mediated by NSAIDs in the gastrointestinal tract has been proposed as one of the key mechanisms underlying their ulcerogenic potential [65]. Thus, impressively, KLS-GABA co-crystal is devoid of the

gastrointestinal side effects that are characteristic of NSAIDs, while it maintains, and also strengthens, their typical therapeutic effects. Taken in the context of NSAID-related side effects, this feature represents a strong advantage of the KLS-GABA co-crystal which can therefore potentially also be administered chronically without incurring gastrointestinal damage.

KLS-GABA co-crystal magnifies the in vivo the synergic effect of the drug-drug combination. Its unique physicochemical characteristics have been shown to improve and accelerate the solubilization process, improving ketoprofen permeability and reducing its contact time with the gastric epithelia. Notably, the inhibition of inducible and constitutive NFκB activation that we observed in the stomachs could also explain the reduction of TNFα and IL-1β expression observed at the spinal level, thus setting the basis for additional studies directed to fully dissect the mechanisms underlying the synergistic action of the combination and the extraordinary potentiation of the in vivo efficacy associated with the co-crystallization of the three components.

Although many studies have finely described how co-crystallization can improve physicochemical properties of different APIs (including NSAIDs) [13], the reports of synergistic pharmacological effects between APIs in drug-drug co-crystals are rare in the literature. The big challenge for the development of pharmaceutically active drug-drug co-crystals is the identification of APIs with complementary or synergic mechanisms of action and appropriate physicochemical characteristics and relative potencies, which could allow for optimal dosing within the stoichiometric constraints created by the co-crystal structure [66]. While few drug-drug co-crystals are currently in the early stage of development for pain treatment [19,66], none are yet available in the market in the pain area, and only one is in late-stage clinical development for the treatment of acute pain [67]. This latter is a co-crystal of tramadol, a synthetic opioid, and celecoxib, an NSAID, (co-crystal of tramadol–celecoxib (CTC)) and has shown modified physicochemical properties [68] and supra-additive antinociceptive effects without additional adverse effects in preclinical and clinical acute pain [69,70]. The results of our studies with the KLS-GABA co-crystal in animal models of inflammatory and neuropathic pain further support the advantages and potential benefits that drug-drug co-crystals can bring to pharmaceutical development and in particular to the treatment of complex multifactorial diseases such as acute, neuropathic and neuroinflammatory pain. KLS-GABA co-crystal is currently in Phase II clinical evaluation, and, in light of its effects in both inflammatory and neuropathic pain models, it is a drug candidate for the treatment of chronic low back pain and other neuroinflammatory conditions.

5. Conclusions

KLS-GABA co-crystal is a new potential therapeutic treatment for chronic pain. It originates from the co-crystallization of ketoprofen, lysine and gabapentin (1:1:1) and has different physicochemical properties and improved pharmacokinetics compared to the mixture of KLS and gabapentin. These features account for the higher gastrointestinal permeability and systemic absorption of the APIs in the co-crystal that, combined with the synergistic action of its components and higher BBB permeation, resulted in greater anti-nociceptive and anti-inflammatory effects in both inflammatory and neuropathic in vivo models. Notably, potentiation of the anti-nociceptive effect was accompanied by a marked increase of the gastrointestinal tolerability of KLS in comparison with the single agents and with the physical combination of the constituent APIs. The synergy between the constituent drugs, which is further boosted by the co-crystallization, allows KLS-GABA co-crystal to reach higher therapeutic efficacy and an improved safety profile at lower dosages of the APIs and thus a potential higher clinical benefit–to–risk ratio. While some aspects of the supra-additive effects of the co-crystal have been defined (i.e., mechanisms underlying the improved gastrointestinal tolerability), the precise factors and mechanisms that are involved and lead to its superior therapeutic efficacy in neuroinflammation and neuropathic pain need to be further investigated and understood. KLS-GABA co-crystal is currently in Phase II clinical evaluation for the treatment of chronic low back pain, and future research will be aimed at more thoroughly investigating its mechanisms of action.

CRediT authorship contribution statement

A.A., G.B. and M.A.: study conceptualization and design, data analysis, interpretation of the results, manuscript writing and review; A.C., L.B.: design and supervision of in vitro, in vivo and ex vivo experiments, interpretation of the results and manuscript review; S.L., M.T.: synthesis of the co-crystal, data acquisition and analysis, interpretation of the results, and manuscript review; N.P., D.C.: co-crystal data acquisition and analysis; P.C.: supervision of animal experiments, interpretation of the in vivo data; R.N.: interpretation of the results, preparation, writing and editing of the manuscript; M.C.D, F.P.: capsules preparation for in vivo experiments; S.Mat.: co-crystal particle aggregation data analysis; S.Bor, M.R.C: solid-state nuclear magnetic resonance of the co-crystal, interpretation of the results and manuscript review; M.dA., V.C., F.dE.: in vitro and ex vivo studies, statistical analysis, interpretation of the results; S.Mai.: manuscript review; L.L.: interpretation of the in vivo results and manuscript review; S.Boc.: in vivo experiments and data analysis, statistical analysis, interpretation of the in vivo results and manuscript review. All authors read and approved the final version of the manuscript.

Declaration of Competing Interest

Aramini A, Bianchini G, Lillini S, Tomassetti M, Cocchiaro P, Novelli R, Dragani MC, Palmerio F, Mattioli S, Boccella S, Brandolini L and Allegretti M are employees of Dompé Farmaceutici S.p.A., Italy. The other authors declare no conflict of interest.

Data Availability

Data will be made available on request. All data supporting the findings of this study are available within the paper and from the corresponding author upon reasonable request.

Acknowledgments

The authors want to deeply thank Prof Annamaria De Luca for her valuable suggestions and contribution in drafting the manuscript.

Appendix A. Supporting information

Supplementary data associated with this article can be found in the online version at doi:10.1016/j.biopha.2023.114845.

References

[1] S.P. Cohen, L. Vase, W.M. Hooten, Chronic pain: an update on burden, best practices, and new advances, Lancet 397 (2021) 2082–2097.
[2] R.R. Myers, W.M. Campana, V.I. Shubayev, The role of neuroinflammation in neuropathic pain: mechanisms and therapeutic targets, Drug Discov. Today 11 (2006) 8–20.
[3] Q. Xu, T.L. Yaksh, A brief comparison of the pathophysiology of inflammatory versus neuropathic pain, Curr. Opin. Anaesthesiol. 24 (2011) 400–407.
[4] R.-R. Ji, Z.-Z. Xu, Y.-J. Gao, Emerging targets in neuroinflammation-driven chronic pain, Nat. Rev. Drug Discov. 13 (2014) 533–548.
[5] P.M. Grace, et al., The neuroimmunology of chronic pain: from rodents to humans, J. Neurosci. 41 (2021) 855–865.
[6] Y.G. Chodakiewitz, G.V.C. Bicalho, J.W. Chodakiewitz, Multi-target neurostimulation for adequate long-term relief of neuropathic and nociceptive chronic pain components, Surg. Neurol. Int. 4 (2013) S170–S175.
[7] E. Cavalli, S. Mammana, F. Nicoletti, P. Bramanti, E. Mazzon, The neuropathic pain: an overview of the current treatment and future therapeutic approaches, Int. J. Immunopathol. Pharmacol. 33 (2058738419838383) (2019).

[8] A. Serrano Afonso, T. Carnaval, S. Videla Cés, Combination therapy for neuropathic pain: a review of recent evidence, J. Clin. Med. 10 (2021) 3533.
[9] J.V. Berger, et al., Cellular and molecular insights into neuropathy-induced pain hypersensitivity for mechanism-based treatment approaches, Brain Res. Rev. 67 (2011) 282–310.
[10] G. Varrassi, et al., Multimodal analgesia in moderate-to-severe pain: a role for a new fixed combination of dexketoprofen and tramadol, Curr. Med. Res. Opin. 33 (2017) 1165–1173.
[11] R.B. Raffa, J.V. Pergolizzi, R.J. Tallarida, The determination and application of fixed-dose analgesic combinations for treating multimodal pain, J. Pain. 11 (2010) 701–709.
[12] L. Song, et al., The effect of combination pharmacotherapy on low back pain: a meta-analysis, Clin. J. Pain. 34 (2018) 1039–1046.
[13] X. Wang, et al., Drug-drug cocrystals: opportunities and challenges, Asian J. Pharm. Sci. 16 (2021) 307–317.
[14] S. Cherukuvada, R. Kaur, T.N.G. Row, Co-crystallization and small molecule crystal form diversity: from pharmaceutical to materials applications, CrystEngComm 18 (2016) 8528–8555.
[15] O.N. Kavanagh, D.M. Croker, G.M. Walker, M.J. Zaworotko, Pharmaceutical cocrystals: from serendipity to design to application, Drug Discov. Today 24 (2019) 796–804.
[16] J. Lu, S. Rohani, Synthesis and preliminary characterization of sulfamethazine-theophylline co-crystal, J. Pharm. Sci. 99 (2010) 4042–4047.
[17] R. Kumar Bandaru, et al., Recent advances in pharmaceutical cocrystals: from bench to market, Front. Pharm. 12 (2021), 780582.
[18] I. Nugrahani, R.D. Parwati, Challenges and progress in nonsteroidal anti-inflammatory drugs co-crystal development, Molecules 26 (2021) 4185.
[19] C. Almansa, C.S. Frampton, J.M. Vela, S. Whitelock, C.R. Plata-Salamán, Co-crystals as a new approach to multimodal analgesia and the treatment of pain, J. Pain. Res. 12 (2019) 2679–2689.
[20] PubChem. Ketoprofen. ⟨https://pubchem.ncbi.nlm.nih.gov/compound/3825⟩.
[21] L. Miles, J. Hall, B. Jenner, R. Addis, S. Hutchings, Predicting rapid analgesic onset of ibuprofen salts compared with ibuprofen acid: Tlag, Tlow, Tmed, and a novel parameter, TCmaxRef, Curr. Med. Res. Opin. 34 (2018) 1483–1490.
[22] R. Altman, B. Bosch, K. Brune, P. Patrignani, C. Young, Advances in NSAID development: evolution of diclofenac products using pharmaceutical technology, Drugs 75 (2015) 859–877.
[23] A. Aramini, et al., Unexpected salt/cocrystal polymorphism of the ketoprofen-lysine system: discovery of a new ketoprofen-L-lysine salt polymorph with different physicochemical and pharmacokinetic properties, Pharm. Basel Switz. 14 (2021) 555.
[24] M.A. Rose, P.C.A. Kam, Gabapentin: pharmacology and its use in pain management, Anaesthesia 57 (2002) 451–462.
[25] V. Vellani, C. Giacomoni, Gabapentin inhibits protein kinase c epsilon translocation in cultured sensory neurons with additive effects when coapplied with paracetamol (Acetaminophen), Sci. World J. 2017 (2017), e3595903.
[26] Y. Narai, N. Imamachi, Y. Saito, Gabapentin augments the antihyperalgesic effects of diclofenac sodium through spinal action in a rat postoperative pain model, Anesth. Analg. 115 (2012) 189–193.
[27] A. Picazo, G. Castañeda-Hernández, M.I. Ortiz, Examination of the interaction between peripheral diclofenac and gabapentin on the 5% formalin test in rats, Life Sci. 79 (2006) 2283–2287.
[28] R.W. Hurley, D. Chatterjea, M. Rose Feng, C.P. Taylor, D.L. Hammond, Gabapentin and pregabalin can interact synergistically with naproxen to produce antihyperalgesia, Anesthesiology 97 (2002) 1263–1273.
[29] L. Brandolini, et al., Paclitaxel binds and activates C5aR1: a new potential therapeutic target for the prevention of chemotherapy-induced peripheral neuropathy and hypersensitivity reactions, Cell Death Dis. 13 (2022) 500.
[30] A. Cimini, et al., Gastroprotective effects of L-lysine salification of ketoprofen in ethanol-injured gastric mucosa, J. Cell. Physiol. 230 (2015) 813–820.
[31] M. Stuart, K. Box, Chasing equilibrium: measuring the intrinsic solubility of weak acids and bases, Anal. Chem. 77 (2005) 983–990.
[32] A. Di Marco, et al., Establishment of an in vitro human blood-brain barrier model derived from induced pluripotent stem cells and comparison to a porcine cell-based system, Cells 9 (2020), E994.
[33] S. Boccella, et al., Preclinical evaluation of the urokinase receptor-derived peptide UPARANT as an anti-inflammatory drug, Inflamm. Res. . J. Eur. Histamine Res. Soc. Al 66 (2017) 701–709.
[34] P. Girard, D. Verniers, M.-C. Coppé, Y. Pansart, J.-M. Gillardin, Nefopam and ketoprofen synergy in rodent models of antinociception, Eur. J. Pharmacol. 584 (2008) 263–271.
[35] T. Librowski, R. Czarnecki, T. Czekaj, H. Marona, New xanthone derivatives as potent anti-inflammatory agents, Med. Kaunas. Lith. 41 (2005) 54–58.
[36] G. Jang, et al., Anti-inflammatory effect of 4,5-dicaffeoylquinic acid on RAW264.7 cells and a rat model of inflammation, Nutrients 13 (2021) 3537.
[37] G.J. Bennett, Y.-K. Xie, A peripheral mononeuropathy in rat that produces disorders of pain sensation like those seen in man, Pain 33 (1988) 87–107.
[38] S.R. Chaplan, F.W. Bach, J.W. Pogrel, J.M. Chung, T.L. Yaksh, Quantitative assessment of tactile allodynia in the rat paw, J. Neurosci. Methods 53 (1994) 55–63.
[39] A. Nsibi, H. Saoud, I. Messaoudi, N.E. Saidi, S. Mani, Unilateral 6-hydroxydopamine-lesioned rat as relevant model to study the pain related to Parkinson's disease, Neurol. Neurobiol. 2019 (2020) 1–5.
[40] C.G. Jolivalt, C.A. Lee, K.M. Ramos, N.A. Calcutt, Allodynia and hyperalgesia in diabetic rats are mediated by GABA and depletion of spinal potassium-chloride co-transporters, Pain 140 (2008) 48–57.
[41] N.B. Eddy, D. Leimbach, Synthetic analgesics. II. Dithienylbutenyl- and dithienylbutylamines, J. Pharmacol. Exp. Ther. 107 (1953) 385–393.
[42] L.O. Randall, J.J. Selitto, A method for measurement of analgesic activity on inflamed tissue, Arch. Int. Pharmacodyn. Ther. 111 (1957) 409–419.
[43] M.A. Ibrahim, W.Y. Abdelzaher, R.R. Rofaeil, S. Abdelwahab, Efficacy and safety of combined low doses of either diclofenac or celecoxib with gabapentin versus their single high dose in treatment of neuropathic pain in rats, Biomed. Pharmacother. 100 (2018) 267–274.
[44] L. Brandolini, et al., Differential protein modulation by ketoprofen and ibuprofen underlines different cellular response by gastric epithelium, J. Cell. Physiol. 233 (2018) 2304–2312.
[45] R. Novelli, et al., Ketoprofen lysine salt has a better gastrointestinal and renal tolerability than ketoprofen acid: a comparative tolerability study in the Beagle dog, Biomed. Pharmacother. 153 (2022), 113336.
[46] M. Gynther, et al., Brain uptake of ketoprofen–lysine prodrug in rats, Int. J. Pharm. 399 (2010) 121–128.
[47] S.-Y. Huang, et al., Sinularin from indigenous soft coral attenuates nociceptive responses and spinal neuroinflammation in carrageenan-induced inflammatory rat model, Mar. Drugs 10 (2012) 1899–1919.
[48] Y. Lu, L.-X. Zhao, D.-L. Cao, Y.-J. Gao, Spinal injection of docosahexaenoic acid attenuates carrageenan-induced inflammatory pain through inhibition of microglia-mediated neuroinflammation in the spinal cord, Neuroscience 241 (2013) 22–31.
[49] I. Gilron, T.S. Jensen, A.H. Dickenson, Combination pharmacotherapy for management of chronic pain: from bench to bedside, Lancet Neurol. 12 (2013) 1084–1095.
[50] R.-R. Ji, A. Nackley, Y. Huh, N. Terrando, W. Maixner, Neuroinflammation and central sensitization in chronic and widespread pain, Anesthesiology 129 (2018) 343–366.
[51] N.B. Torres, C. Altafini, Drug combinatorics and side effect estimation on the signed human drug-target network, BMC Syst. Biol. 10 (2016) 74.
[52] K.T. Velázquez, H. Mohammad, S.M. Sweitzer, Protein kinase C in pain: Involvement of multiple isoforms, Pharmacol. Res. 55 (2007) 578–589.
[53] S. Emami, M. Siahi-Shadbad, K. Adibkia, M. Barzegar-Jalali, Recent advances in improving oral drug bioavailability by cocrystals, BioImpacts BI 8 (2018) 305–320.
[54] H.R. Guzmán, et al., Combined use of crystalline salt forms and precipitation inhibitors to improve oral absorption of celecoxib from solid oral formulations, J. Pharm. Sci. 96 (2007) 2686–2702.
[55] K. Kawakami, Theory and practice of supersaturatable formulations for poorly soluble drugs, Ther. Deliv. 6 (2015) 339–352.
[56] A. Alhalaweh, H.R.H. Ali, S.P. Velaga, Effects of polymer and surfactant on the dissolution and transformation profiles of cocrystals in aqueous media, Cryst. Growth Des. 14 (2014) 643–648.
[57] Z. Huang, S. Staufenbiel, R. Bodmeier, Kinetic solubility improvement and influence of polymers on controlled supersaturation of itraconazole-succinic acid nano-co-crystals, Int. J. Pharm. 616 (2022), 121536.
[58] Y. Zhang, X. Du, H. Wang, Z. He, H. Liu, Sacubitril-valsartan cocrystal revisited: role of polymer excipients in the formulation, Expert Opin. Drug Deliv. 18 (2021) 515–526.
[59] N. Hisada, et al., Characterizing the dissolution profiles of supersaturable salts, cocrystals, and solvates to enhance in vivo oral absorption, Eur. J. Pharm. Biopharm. . J. Arb. Pharm. Verfahr. EV 103 (2016) 192–199.
[60] K. Pohóczky, et al., Discovery of novel targets in a complex regional pain syndrome mouse model by transcriptomics: TNF and JAK-STAT pathways, Pharmacol. Res. 182 (2022), 106347.
[61] K.O. Aley, R.O. Messing, D. Mochly-Rosen, J.D. Levine, Chronic hypersensitivity for inflammatory nociceptor sensitization mediated by the ε isozyme of protein kinase C, J. Neurosci. 20 (2000) 4680–4685.
[62] C.A. Parada, J.J. Yeh, E.K. Joseph, J.D. Levine, Tumor necrosis factor receptor type-1 in sensory neurons contributes to induction of chronic enhancement of inflammatory hyperalgesia in rat, Eur. J. Neurosci. 17 (2003) 1847–1852.
[63] M.M. Campos, G.E. Souza, J.B. Calixto, In vivo B1 kinin-receptor upregulation. Evidence for involvement of protein kinases and nuclear factor kappaB pathways, Br. J. Pharm. 127 (1999) 1851–1859.
[64] N. Malek, A. Pajak, N. Kolosowska, M. Kucharczyk, K. Starowicz, The importance of TRPV1-sensitisation factors for the development of neuropathic pain, Mol. Cell. Neurosci. 65 (2015) 1–10.
[65] J.L. Wallace, Prostaglandins, NSAIDs, and gastric mucosal protection: why doesn't the stomach digest itself? Physiol. Rev. 88 (2008) 1547–1565.
[66] C. De Palma, et al., Ibuprofen–arginine generates nitric oxide and has enhanced anti-inflammatory effects, Pharmacol. Res 60 (2009) 221–228.
[67] R. Thipparaboina, D. Kumar, R.B. Chavan, N.R. Shastri, Multidrug co-crystals: towards the development of effective therapeutic hybrids, Drug Discov. Today 21 (2016) 481–490.
[68] J. López-Cedrún, et al., Co-crystal of tramadol-celecoxib in patients with moderate to severe acute post-surgical oral pain: a dose-finding, randomised, double-blind, placebo- and active-controlled, multicentre, phase II trial, Drugs RD 18 (2018) 137–148.
[69] C. Almansa, et al., Co-crystal of tramadol hydrochloride–celecoxib (ctc): a novel API–API Co-crystal for the treatment of pain, Cryst. Growth Des. 17 (2017) 1884–1892.
[70] M. Merlos, et al., Administration of a co-crystal of tramadol and celecoxib in a 1:1 molecular ratio produces synergistic antinociceptive effects in a postoperative pain model in rats, Eur. J. Pharmacol. 833 (2018) 370–378.